

STUD GROUPS LOADED IN SHEAR

By

TEE LIANG WONG

Bachelor of Science in Civil Engineering

Oklahoma State University

Stillwater, Oklahoma

1987

Submitted to the Faculty of the
Graduate College of the
Oklahoma State University
in partial fulfillment of
the requirements for
the Degree of
MASTER OF SCIENCE
December, 1988

YOUNG, R. L. (1988)

Thesis
1988
W8715
cop. 2

STUD GROUPS LOADED IN SHEAR

Thesis Approved:

R. C. Donaley

Thesis Adviser

Gerald D. Oberlander

John B. Lloyd

Norman N. Durham

Dean of the Graduate College

ACKNOWLEDGEMENTS

The author wishes to express his sincere gratitude and appreciation to all the people who have helped make this investigation possible.

Dr. Rex C. Donahey, who served as chairman of the Graduate Committee, for obtaining the PCI Fellowship, his excellent guidance, invaluable suggestions, generous encouragement, and help at all stages of this investigation.

Dr. Garold D. Oberlender and Dr. John P. Lloyd for their assistance and advise while serving on the author's committee.

Mr. Herman C. Himes of Thomas Concrete Products in Oklahoma City for his help in fabricating the test specimens. Nelson Stud Welding Division of Lorain, Ohio, for supplying the shear studs.

Dr. Allen E. Kelly, Dr. William P. Dawkins, and Dr. Farrel J. Zwerneman for their excellent instructions throughout my study at Oklahoma State University.

Mr. William D. Spoonemore, Mr. Kim Aik Yap, Mr. Chuan Heng Er, and friends for their help in the fabrication of the slabs and assistance during the testing stage. Mr. M. Senthil Kumar, for reading and editing the thesis.

The author is greatly indebted to his wife, Yi-Cheng Lim, for her love, understanding, patience, help, and support

throughout my graduate study.

This thesis is dedicated to my parents, Mr. and Mrs. Bok-Dat Wong, for their love, sacrifice, support, and encouragement.

TABLE OF CONTENTS

Chapter	Page
I. INTRODUCTION	1
1.1 Statement of the Problem	1
1.2 Previous Work	2
1.2.1 Studs Loaded in Tension	2
1.2.2 Studs Loaded in Shear	5
1.2.3 Studs Loaded in Combined Tension and Shear	14
1.3 Object and Scope	18
II. EXPERIMENTAL PROGRAM	20
2.1 Introduction	20
2.2 Materials	20
2.2.1 Test Specimens	20
2.2.2 Concrete Slabs	22
2.2.3 Hairpin Reinforcement	23
2.3 Test Apparatus	23
2.4 Test Procedure	24
2.5 Test Results	25
2.5.1 General	25
2.5.2 Type I Specimens	26
2.5.3 Type II Specimens	27
2.5.4 Type III Specimens	27
III. ANALYSIS AND DISCUSSION	29
3.1 General	29
3.2 Evaluation of Test Results	29
3.2.1 Effect of Edge Distance	29
3.2.2 Effect of Corner Distance	30
3.2.3 Effect of Embedment Length	31
3.2.4 Effect of Stud Spacing and Group Width	32
3.2.5 Effect of Front Row Studs	32
3.2.6 Effect of Slab Thickness	33
3.2.7 Effect of Casting Position	33
3.2.8 Effect of Hairpin Reinforcement	34
3.3 Empirical Design Equations	35
3.3.1 Type I Specimens	36
3.3.2 Type II Specimens	38

Chapter	Page
IV. SUMMARY AND CONCLUSIONS	41
4.1 Summary	41
4.2 Conclusions	41
4.3 Future Work	43
A SELECTED BIBLIOGRAPHY	45
APPENDIX A: TABLES	47
APPENDIX B: FIGURES	52
APPENDIX C: SHEAR TEST DATA (12)	89
APPENDIX D: CRUZ'S EXPERIMENTAL DATA (17)	92
APPENDIX E: PREDICTED LOAD VERSUS TEST LOAD FOR TYPE I SPECIMENS	94

LIST OF TABLES

Table	Page
I. Stud Specification	48
II. Properties of Concrete	49
III. Specimens Specification	50
IV. Test Results	51

LIST OF FIGURES

Figure	Page
1 Pullout Failure for Concrete Loaded in Tension (8)	53
2 Pullout Surface Areas for Stud Groups (7)	54
3 Stud Groups in Tension (5)	55
4 Concrete Placement Direction (13)	56
5 Suggested Method of Placement for Hairpin Reinforcement (15)	56
6 Various Types of Specimens with Corresponding Loading Direction	57
7 Configurations of Stud Groups	58
8 Details of Specimen with Hairpin Reinforcement	59
9 Position of Stud Groups	60
10 Position of PVC Pipe and Concrete Inserts	61
11 Test Apparatus (Plan)	62
12 Test Apparatus (Section)	63
13 Semi-conical Failure Mode for Type I Specimen Embedded in "Thick" Slab	64
14 Load-Slip Curves for Type I Specimens Embedded in "Thick" Slabs	65
15a Failure Pattern for Type I Specimens Embedded in "Thin" Slabs	66
15b Failure Pattern for Type I Specimens Embedded in "Thin" Slabs	67
16 Load-Slip Curves for Type I Specimens Embedded in 4 in. Slabs	68

Figure	Page
17 Load-Slip Curves for Type I Specimens Embedded in 8 in. Slabs	68
18 Load-Slip Curves for Type I Specimens with Hairpin Reinforcement	69
19 Type I Specimens with Hairpin Reinforcement	70
20 Failure Pattern for Type II Specimens Embedded in "Thick" Slabs	71
21 Failure Pattern for Type II Specimens Embedded in "Thin" Slabs	72
22 Load-Slip Curves for Type II Specimens Embedded in 12 in. and 8 in. Slabs	73
23 Load-Slip Curves for Type II Specimens Embedded in 4 in. Slabs	73
24 Load-Slip Curves for Type II Specimens Embedded in 8 in. Slabs	74
25 Failure Pattern for Type III Specimens	75
26 Load-Slip Curves for Type III Specimens	76
27 Stud Group Schematic	76
28 Effect of Edge Distance on Ultimate Test Load for Type I Specimens with 6 in. Stud Spacing	77
29 Effect of Edge Distance on Ultimate Test Load for Type I and II Specimens in 4, 8, and 12 in. Slabs with 6 in. Stud Spacing	77
30 Effect of Edge Distance on Ultimate Test Load for Type III Specimens with 4 in. Stud Spacing	78
31 Effect of Corner Distance on Ultimate Test Load for Specimens Embedded in 4 and 8 in. Slabs	78
32 Ratio of Type I to Type II Ultimate Test Load versus Edge Distance	79
33 Shear Cone Pullout for a Partially Embedded Stud (19)	79
34 Effect of Embedment Length on Ultimate Test Load for Type I Specimens with Two Rows of Studs (17)	80

Figure	Page
35 Ratio of Long Stud to Short Stud Ultimate Test Load versus Edge Distance (17)	80
36 Effect of Embedment Length on Ultimate Test Load for Type III Specimens with 2 in. Stud Spacing (17). .	81
37 Ratio of Long Stud to Short Stud Ultimate Test Load versus Edge Distance for Type III Specimens with 2 in. Stud Spacing (17)	81
38 Effect of Lateral Stud Spacing on Ultimate Test Load for Type I and II Specimens with 5 in. Edge Distance	82
39 Effect of Front Row Studs on Ultimate Test Load for Type I Specimens with 2 in. Stud Spacing (17) . .	82
40 Ratio of Ultimate Test Load for Specimens with Two Rows of Studs to Specimens with One Row versus Number of Studs Per Row (17)	83
41 Effect of Slab Thickness on Ultimate Test Load for Type III Specimens with 2 in. Stud Spacing	83
42 Effect of Casting Position on Ultimate Test Load for Type I Specimens Embedded in 8 in. Slabs with 6 in. Stud Spacing	84
43 Ratio of Bottom-Mounted Stud Group to Top-Mounted Stud Groups Ultimate Test Load versus Edge Distance	84
44 Load-Slip Curves for Type I Specimens with (1B, 4B, and 2C) and without (3B, 5B, and 3C) Hairpin Reinforcement Embedded in 4 and 8 in. Slabs . . .	85
45 Failure Surface for Type I Specimens Embedded in "Thick" Slabs	85
46 Failure Surface for Type I Specimens Embedded in "Thin" Slabs	86
47 Failure Surface for Type II Specimens Embedded in "Thick" Slabs	86
48 Failure Surface for Type II Specimens Embedded in "Thin" Slabs	87
49 Comparison of Calculated Loads from Eq. 3.4, 3.6, 3.9, and 3.10 with Ultimate Test Loads	87

Figure	Page
50 Comparison of Calculated Loads from Proposed Empirical Equations with Ultimate Test Loads	88
51 Comparison of Calculated Loads for Type I Specimens Using the PCI Procedure (7) and Proposed Empirical Equations	88

NOMENCLATURE

d	stud diameter (in.)
d_c	corner distance (in.)
d_e	edge distance (in.)
f'_c	compressive strength (psi)
l_e	embedment length (in.)
n	number of studs in rear row
S_x	lateral stud spacing (in.)
S_y	longitudinal stud spacing (in.)
t	slab thickness (in.)
V_n	nominal shear strength (lb.)
V_{nc}	nominal shear strength with corner effect (lb.)

CHAPTER I

INTRODUCTION

1.1 Statement of the Problem

Concrete structures, whether precast or cast-in-place, often require the use of embedded-plate connections. The plates are anchored to the concrete using deformed bar anchors or headed studs and are, in turn, connected to other elements of the structure by welding or bolting.

Because headed studs are compact, easily installed, and of consistent quality, they have become widely accepted. A large number of studies (2, 12, 15, and 17) have shown, however, that connections made with headed studs or anchor bolts tend to fail in a brittle manner in the concrete especially when the connectors are located near a free edge. It is important, therefore, that connection capacities are accurately determined.

A large number of tests of single-stud and multiple-stud connections loaded in tension have been conducted (1, 2, 10, and 16).

Although there have been a number of studies into the behavior and strength of headed studs loaded in shear, these studies have primarily concentrated on the behavior of single headed stud. In many applications, however, stud groups are

common. Additional testing of stud groups and reevaluation of the existing design procedures are therefore required.

1.2 Previous Work

1.2.1 Studs Loaded in Tension

1.2.1.1 Experimental Work. Bode and Roik (1) studied the tensile strength of single stud and stud group connections embedded in normal weight concrete. The concrete blocks used in their investigation were sufficiently large to eliminate edge effects. Of the 150 tests that were conducted, results of 106 tests were selected to establish the following design equation:

$$\max T = F(h_s \beta_w)^{1/4} (h_s + d_2) \quad (1.1)$$

where:

$\max T$ = tensile strength (N)

F = non-dimensional coefficient to determine the tensile strength, calculated from test results

h_s = embedded shaft length (mm)

d_2 = diameter of stud head (mm)

β_w = cube strength of concrete (N/mm²).

Hawkins (2) studied the strength of cast-in-place anchor bolts loaded in shear and tension. Twelve specimens were used in the tensile tests. The variables used in the investigation were anchor embedment length (3, 5, and 7 in.); anchor washer diameter (2, 4, and 6 in.); and washer thickness (5/8 and 7/8 in.). The bolt diameter was one inch for all the tests. Two failure modes were observed; namely,

shear cone pullout failure, C, and radial cracking failure, R.

According to Hawkins, the failure mode was primarily governed by the embedment length of the bolt. He observed type C failures for shallow embedment lengths and type R failures for deep embedment lengths of bolts. He concluded that splitting failure was possible when the depth-to-diameter ratio of a bolt exceeded four. Anchor plates at the bolt heads were found to increase the diameter of the shear cone for pullout type failures. The pullout strength was therefore increased.

1.2.1.2 Empirical Design Equations. Studs embedded in concrete and loaded in tension generally fail in two modes. In the first mode, the concrete fails in tension. A conical failure surface forms at an angle, α , relative to the stud as shown in Figure 1. For design purposes, it is normally assumed that α is equal to 45 degrees. In the second mode, the stud yields in tension. The failure mode is primarily a function of the embedment length of the stud. When concrete failure occurs, the stud is considered to be partially developed, while when stud failure occurs, the stud is considered to be fully developed.

A number of design equations have been proposed for both failure modes. For partially embedded studs, Prestressed Concrete Institute (PCI) Connection Manual (3) and KSM Engineering Aspect (4) suggest that the ultimate pullout strength for a single stud is given by:

$$P'_{uc} = 17.8\phi(l_e + d_h)\sqrt{f'_c}l_e \quad (1.2)$$

where ϕ = strength reduction factor = 0.85

l_e = embedment length (in.)

d_h = diameter of stud head (in.)

f'_c = concrete compressive strength (psi).

Shaikh and Yi (5) and ACI Committee 349 (6) recommend that the lower bound capacity of a single stud is given by:

$$\phi P_c = \phi 2.8\lambda\sqrt{f'_c}A_o \quad (1.3)$$

where ϕ = strength reduction factor = 0.85

λ = concrete type factor = 1.0 for normal weight concrete, 0.85 for sand lightweight concrete and 0.75 for all lightweight concrete

A_o = area of the assumed failure surface which, for a stud not located near a free edge, is taken to be that of a 45 degree cone.

$$= \sqrt{2}\pi l_e(l_e + d_h). \quad (1.3A)$$

Multiple studs are often welded on a plate to act as a group. The PCI Design Handbook (7) indicates that the failure surface for a stud group loaded in tension is likely to be a truncated pyramid (Figure 2). For different stud patterns and boundary conditions, Shaikh and Yi (5) list the corresponding tensile strength design equations as shown in Figure 3.

According to the Nelson Design Data 10 (8) and PCI Design Handbook (7), full embedment length for single stud is in the range of 8 to 10 times the anchor shank diameter. The tensile strength of a fully embedded stud, P'_{ue} , is defined

as:

$$P'_{ue} = 0.9A_S f_S \quad (1.4)$$

where:

A_S = cross sectional area of the anchor shank (in²)

f_S = tensile strength of the anchor steel (ksi).

The presence of a free edge adjacent to a stud loaded in tension has the effect of reducing the tensile capacity of the connection by a) reducing the surface area and b) reducing the available tensile capacity of the concrete (5).

Many design procedures propose the use of a truncated cone failure surface to compute the tensile capacity of the connection located near a free edge. In addition, an edge effect reduction factor, K'_e , which accounts for the reduced tensile capacity of the concrete, is recommended (6, 8, 9, and 10). Shaikh and Yi (5) recommend the following equations for K'_e , and pullout strength, P_{uc} , for a connector in the vicinity of a free edge:

$$K'_e = \frac{4}{\sqrt{2}} \left[\frac{2A_{po}}{A_o} - 1 \right] \quad (1.5)$$

$$P_{uc} = \frac{4}{\sqrt{2}} \sqrt{f'_c} A_o \left[\frac{2A_{po}}{A_o} - 1 \right] \quad (1.5A)$$

$$\frac{A_{po}}{A_o} \leq 1.0 \quad (1.5B)$$

where:

f'_c = concrete compressive strength (psi)

A_0 = full cone surface area

A_{po} = partial cone surface area.

1.2.2 Studs Loaded in Shear

1.2.2.1 Experimental Work. In 1971, Ollgaard, Slutter, and Fisher (11) investigated the shear strength of stud connectors in lightweight and normal weight concrete. Forty-eight pushout tests were conducted to study various parameters such as concrete compressive strength, split tensile strength, modulus of elasticity, density, stud diameter, type of aggregate, and number of connectors per slab. Two types of coarse aggregate (crushed limestone and natural river gravel) were used for normal weight concrete. Lightweight concrete was made of three types of lightweight aggregate: Type C, D, and E. Type C aggregate consisted of rounded expanded shale with a maximum size of 1/2 in.; type D aggregate consisted of irregular expanded shale with a maximum size of 3/4 in.; type E aggregate consisted of irregular expanded slate with a maximum size of 3/4 in.

Two failure modes -- concrete shear cone pullout and stud failure, were observed in the tests. All the studs were located far away from the free edge and all failures were in the concrete. Ollgaard, Slutter, and Fisher (11) conclude that the compressive strength and modulus elasticity of concrete are the major factors affecting the shear capacity of stud connectors embedded in both normal weight and lightweight concrete. Based on a regression analysis of the

test data, the shear strength, in kips, is given by:

$$Q_u = 1.106 A_s f'_c{}^{0.3} E_c{}^{0.44} \quad (1.6)$$

where:

A_s = cross-sectional area of shear stud connector
(in.²)

f'_c = concrete compressive strength (Ksi)

E_c = modulus of elasticity (Ksi).

For design purposes, Eq. 1.6 can be simplified to:

$$Q_u = \frac{1}{2} A_s (f'_c E_c)^{\frac{1}{2}} \quad (1.7)$$

Cannon, Burdette, and Funk (12) conducted shear tests on 54 specimens with modified inserts, studs, and bolts of various diameters embedded in normal weight concrete. The various anchor patterns and test data are listed in Appendix C. The authors found that boundary condition, strength of concrete, size, strength, number, and spacing of anchors controlled the anchorage requirements.

Cannon et al concluded that the embedment requirements are related to the concrete and anchoring conditions of bolts. The edge condition was shown to have an important effect on the ultimate strength of the anchors. The shear strength of bolted connections was primarily affected by the strength of bolts and by the method of attachment. It was recommended that the shear capacity should be reduced for bolts and anchors with a free edge located closer than 1.25 times the required embedment length (usually 8-bolt diameters). Also, the authors discourage the use of anchor plates at bolt heads as they tend to: a) increase the

anchorage depth to avoid shear cone pullout and b) reduce the concrete tensile strength between the bolt heads caused by loss of direct concrete bonding. The following equation was proposed for the nominal shear failure load, limited by concrete failure, of an individual bolt :

$$V_c = 2\pi\sqrt{f'_c} \left[\frac{(m + d/2)}{\tan\phi} \right]^2 \quad (1.8)$$

where:

f'_c = concrete compressive strength (psi)

$\phi = (m + d/2)^4 + 25 \text{ deg.} \leq 45 \text{ deg.}$

m = edge distance (in.)

d = bolt diameter (in.).

Hawkins (2) conducted shear tests on fifteen anchor bolt specimens with embedment lengths of 3 in. and 5 in.. The failure modes of the shear tests were classified as radial failure and shear cone pullout failure. Shear cone pullout occurred only in the case of specimens with a 3-in. embedment depth. The presence of reinforcement did not improve the resistance of concrete to radial failure. The test results show that the stiffness of an anchor bolt is related to $\sqrt{f'_c}$ and $\sqrt[3]{d_b}$, where d_b is the diameter of the bolt, rather than the embedment depth or the washer diameter. When a washer was used in the specimen, shear strength increased gradually with an increase in embedment length. Based on Hawkins' statistical analysis, the following empirical equation was proposed for specimens without edge effects:

$$V_u = 18.2\sqrt{f'_c}^3\sqrt{d_b}(15 + 1.1L_e + d_w) \quad (1.9)$$

where:

V_u = shear strength (lbs.)

L_e = embedment length (in.)

d_w = washer diameter (in.) $\leq L_e$

d_b = bolt diameter (in.).

The ultimate capacity of the specimens, limited by the shearing yield strength of the bolts, was assumed to be:

$$V_u = \frac{0.6\pi d_b^2 f_y}{4} = 0.47d_b^2 f_y \quad (1.10)$$

where:

f_y = bolt yield strength (psi).

A splitting type of failure was observed in the case of specimens with large embedment lengths. These splitting failures imposed a limiting ultimate capacity on the specimens, regardless of the embedment length. Hawkins noticed that anchor plates only improved the ultimate shear capacity of those specimens that failed in shear cone pullout. It was shown that the ultimate shear capacity of an anchor bolt connector limited by steel failure is about 20 to 30 percent less than that of a headed stud connector of comparable size. In addition, the slip of anchor bolts under shear load was shown to be much greater than the slip of stud connectors. These differences was primarily due to the inadequate fixity in the connection.

Often, the shear strength of headed studs is influenced by the direction of the concrete placement. Maeda, Matsui,

and Hiragi (13) investigated the effect of concrete placement on the shear strength of headed studs. Four placement directions were considered: a) downward placement against studs standing upward (A-type), b) downward placement with the studs upside down (B-type), c) downward placement with the studs fixed horizontally (C-type; with bleeding occurring at the bearing side), and d) downward placement with studs placed horizontally but loaded at 90 degree from the bleeding side (D-type) as shown in Figure 4.

Critical load is defined as the capacity of the specimen when it reaches a residual slip of value 0.075 mm. Maeda et al observed that A-type specimens had the highest critical load while C-type specimens exhibited the lowest critical load. It was also observed that the effect of bleeding became insignificant at ultimate load capacity in all specimens. The following equation was proposed for the nominal static strength of studs, Q_u , for all types of specimens:

$$Q_u = 40DH\sqrt{\sigma_{ck}} \quad (1.11)$$

where:

D = diameter of stud (cm)

H = height of stud (cm)

σ_{ck} = design strength of concrete (kgf/cm²).

The strength at serviceability limit, Q_s , was found to be a function of placement direction.

For A, B, and D type placements:

$$Q_s = 0.5Q_u \quad (1.12)$$

and for C type placement:

$$Q_s = 0.35Q_u. \quad (1.13)$$

Kuhn and Buckner (14) conducted tests similar to those by Maeda et al. The test specimens were classified as BOTTOM, SIDE, TOP LOOSE, and TOP FIXED. BOTTOM specimens were cast with 16 in. of concrete above the embedment plate. The average slump of the concrete was 4 in.. Concrete was placed in the forms and consolidated by vibration. SIDE specimens were cast with the plate positioned on the side of the concrete slab with 8 in. of concrete below the studs. TOP LOOSE specimens were fabricated by placing the embedment plate in after the forms were filled. Lastly, TOP FIXED specimens were cast with the plate initially secured to the formwork. All specimens failed in the stud shanks except one TOP LOOSE specimen. It was observed that the BOTTOM and SIDE specimens had smooth and uniform surfaces beneath the concrete plates, indicating good concrete consolidation. However, in the TOP FIXED specimens, 50% of the surface area was filled with large air voids. The TOP LOOSE specimens exhibited better surface contact, with approximately 25% air voids. The shear capacities of the BOTTOM specimens were about 30% higher than those of the TOP specimens. The differences in characteristics between the TOP FIXED and TOP LOOSE specimens were insignificant.

Klingner, Mendonca, and Malik (15) investigated the effect of hairpin reinforcement on the failure characteristics and ultimate load of the single shear

connector located near a free edge. Their investigation included 3/4-in. diameter A307 anchor bolts embedded in normal weight concrete loaded with monotonic or cyclic loads. A total of 56 anchor bolts with an 8-in. embedment lengths were tested. The parameters investigated included surface condition, loading plate size, and edge distance. Three surface conditions between the concrete and the loading plate were prepared: normal (steel troweled, no curing compound); a thin, sand-cement mortar coating; and a Teflon sheet. Two loading plate sizes, 6 x 6 in. and 12 x 12 in., were used. The edge distance varied from 2 in. to 12 in.

The authors observed that specimens loaded with different plate sizes had identical ultimate loads. The failure loads for specimens with normal surfaces were 5 and 10 percent higher than for specimens with mortar and Teflon surfaces respectively.

The authors found that the test data correlated well with the following static load equation for specimens limited by concrete failure:

$$V_c = 2\pi d_e^2 \sqrt{f'_c} \quad (1.14)$$

where:

d_e = edge distance (in.)

f'_c = concrete compressive strength (psi).

If the above equation is to be used for design purposes, the authors suggest a 35 percent reduction in the shear capacity of Eq. 1.14. The design shear strength of anchorages, based on steel failure is:

$$\phi_s V_s = \phi_s A_s (0.75 f_{ut}) \quad (1.15)$$

where:

ϕ_s = strength reduction factor = 0.90, and

f_{ut} = specified minimum ultimate tensile strength of anchor.

The authors recommend that hairpins used to resist shear load should be placed close to the applied load and directly against the connector as shown in Figure 5.

1.2.2.2 Empirical Design Equations. PCI Design

Handbook (7) suggests that the design shear strength governed by concrete failure, ϕV_c , should be taken as the least of the values given by the following equations:

$$\phi V_c = \phi 800 A_p \lambda \sqrt{f'_c} \quad (1.16)$$

$$\phi V_c = \phi 2 \pi d_e^2 \lambda \sqrt{f'_c} \quad (1.17)$$

where:

ϕ = 0.85

A_p = cross sectional area of steel

λ = 1.0 for normal weight concrete, 0.85 for sand lightweight concrete and 0.75 for all lightweight concrete.

The design shear strength for stud groups based on concrete failure should be taken as the least of:

1. Strength of the weakest stud, based on the above equations, times the number of studs,
2. Strength based on d_e of the weakest row of studs times the number of rows, or
3. Strength based on d_e of the row of studs farthest from

the free edge.

However, no test data were cited to support this recommendation.

1.2.3 Studs loaded in Combined Tension and Shear

1.2.3.1 Experimental Work. McMackin, Slutter, and Fisher (16) studied the effects of combined tension and shear on studs embedded in normal weight and lightweight concrete. Studs of 3/4- and 7/8-in. diameter with 4 to 8 in. embedment length were tested with three different loading conditions. Additional 3/4-in. diameter specimens located near a free edge were tested in pure tension and pure shear.

The parameters that were included in these tests were the type of concrete, embedment length, angle of loading, and free edge distance. Two different loading angles, 30 degrees and 60 degrees, were used in the combined loading tests. The specimens were categorized as: a) anchors with full embedment in normal weight concrete; b) anchors with full embedment in lightweight concrete; and c) anchors with partial embedment in normal weight concrete.

The three failure patterns observed were failure of the stud anchor, severe concrete cracking, and concrete cone pullout. The test data indicate that, for conditions (a) and (b) as described above, the interaction between tension and shear is given by:

$$\left[\frac{P}{P_u} \right]^{5/3} + \left[\frac{S}{S_u} \right]^{5/3} \leq 1.0 \quad (1.18)$$

where:

P = applied tension load

S = applied shear load

$$P_u = \sigma_u A_s = 60 A_s \quad (1.18a)$$

$$S_u = 1.106 A_s f'_c{}^{0.3} E_c{}^{0.44} \leq 60 A_s \quad (1.18b)$$

A_s = cross-sectional area of anchors

σ_u = steel tensile strength.

For partially embedded specimens in normal weight concrete (condition C), the following expression is recommended:

$$\left[\frac{P}{P_{cu}} \right]^{5/3} + \left[\frac{S}{S_u} \right]^{5/3} \leq 1.0 \quad (1.19)$$

where:

$$P_{cu} = 0.56C(L_e + d_h)L_e\sqrt{f'_c} \leq \sigma_u A_s \quad (1.19a)$$

L_e = embedment length (in.)

d_h = head diameter (in.)

C = 0.75 for all lightweight concrete

= 0.85 for sanded lightweight concrete

= 1.0 for normal weight concrete

A strength design equation can be obtained from Eq. 1.19 by multiplying a φ factor of 0.85.

1.2.3.2 Empirical Design Equations. PCI Connection

Manual (3) recommends the following design equation for

specimens loaded with combined tension and shear which is limited by the concrete capacity:

$$\left[\frac{P_u}{P'_{uc}} \right]^{4/3} + \left[\frac{V_u}{V'_{uc}} \right]^{4/3} \leq 1.0 \quad (1.20)$$

where:

P_u = applied tension load

V_u = applied shear load

$P'_{uc} = 17.8\phi(l_e + d_h)l_e\sqrt{f'_c}$

$V'_{uc} = \phi(2500d_e - 3500) \quad (1.20a)$

$\phi = 0.85$

l_e = embedment length (in.)

d_h = head diameter of anchor (in.)

f'_c = concrete compressive strength (psi.)

KSM Engineering Aspects (4) also recommends the same design equation but defines V'_{uc} as follows:

$$V'_{uc} = \phi\mu P'_{uc} \quad (1.20b)$$

where:

$\phi = 0.85$

$$\mu = \frac{300}{pf_y} + 0.5 \leq 1 \quad (1.20c)$$

$$p = \frac{a_s}{A_c} \quad (1.20d)$$

f_y = yield stress of steel = $0.9f'_s = 54000$ psi

a_s = shank area per anchor (in.²)

$$A_c = 0.25\pi(2l_e + d_h)^2 \quad (1.20e)$$

For headed-stud connections, governed by the steel

strength, the following interaction equation is recommended
(4):

$$\left[\frac{P_{us}}{P'_{us}} \right]^2 + \left[\frac{V_{us}}{V'_{us}} \right]^2 \leq 1.0 \quad (1.21)$$

where:

P_{us} = applied ultimate tension load

V_{us} = applied ultimate shear load

P'_{us} = ultimate steel tensile capacity = $0.9A_p f_s$

V'_{us} = ultimate steel shear capacity = $0.75A_p f_s$

f_s = steel tensile strength = 60000 psi

The PCI Design Handbook (7) defines the interaction equation for combined loading as:

$$\text{Concrete: } \frac{1}{\phi} \left[\left[\frac{P_u}{P_c} \right]^2 + \left[\frac{V_u}{V_c} \right]^2 \right] \leq 1.0 \quad (1.22)$$

where:

$\phi = 0.85$

P_u and V_u = factored tension and shear capacities

P_c and V_c = nominal tension and shear capacities of
concrete.

According to Shaikh and Yi (5), it is more appropriate to place the factor ϕ outside the exponent to avoid multiplying the lower strength reduction factor twice, for example, $\phi = 0.85$ and $\phi^2 = 0.72$.

$$\text{Steel: } \frac{1}{\phi} \left[\left[\frac{P_u}{P_s} \right]^2 + \left[\frac{V_u}{V_s} \right]^2 \right] \leq 1.0 \quad (1.23)$$

where:

$$\phi = 1.0$$

P_s and V_s = tensile and shear strength of steel.

Shaikh and Yi also recommend that the design strength of studs under combined tension and shear should satisfy Eq. 1.22 and 1.23.

1.3 Object and Scope

The objective of this study is to investigate the behavior of embedded stud groups loaded in shear. The study concentrates on the following parameters: edge distance, lateral stud spacing and group width, corner distance, embedment length, slab thickness, casting position, and supplemental reinforcement. Based on the experimental work conducted in the investigation, empirical design equations are presented.

Thirty-three specimens were embedded in normal weight concrete and tested to failure. These specimens were classified as Type I, II, and III. Specimens Type I and II were loaded in pure shear toward a free edge. Specimens Type III were loaded in shear and torsion with the load applied parallel to the free edge. Load-slip curves were obtained from each test. Test data obtained from this study will be combined with test data from Cruz's report, titled "Effect of

Edge Distance on Stud Groups Loaded in Shear and Torsion"

(17), for analysis. Regression analyses were used to evaluate the test data and to establish empirical equations for the nominal shear strength of stud groups. Calculated shear strengths based on the PCI design procedure (7) were compared with the test data.

CHAPTER II

EXPERIMENTAL PROGRAM

2.1 Introduction

Three specimen types, as shown in Figure 6, were tested in this investigation. Type I specimens were embedded in concrete near a free edge and were loaded in shear towards the free edge. Type II specimens were placed near a corner and were loaded in shear towards the free edge. Type III specimens comprised connections loaded with combined torsion and shear. The shear load was applied parallel to the free edge.

2.2 Materials

2.2.1 Test Specimens

Thirty-three specimens were used in the current investigation. All of the test specimens were fabricated using 1/2-in. diameter Nelson studs welded on one side of 3/8-in. steel plates. The plate thickness was selected according to the PCI Design Handbook (7), which specifies the minimum plate thickness to be at least 2/3 of the stud diameter. All the studs were supplied by the Nelson Stud Welding Division of TRW. To ensure uniformity in the stud

properties, all the studs were taken from the same lot. The stud properties are listed in Table I. Based on Cruz's work (17), which indicated minimal effect of stud length on shear capacity, two-inch long studs were selected for the current investigation. The different configurations of the stud groups are shown in Figure 7. Four specimens had hairpin reinforcement (see Figure 8).

Three specimen types were used: Type I, II, and III. Seventeen Type I specimens were tested in this study. Each of these specimens was embedded in concrete with only one free edge located in the direction of applied load as shown in Figure 6.

Two specimens from the 12 in. slab were used to duplicate Cruz's specimens (17), to:

- 1) compare the test results;
- 2) prove that the data collected by Cruz were not affected by the steel channel that was used as part of the load bearing frame.

Specimens 6B and 6C from the current investigation were compared with specimens 8 and 7 from Cruz's experiment as shown in Appendix D.

All the plates, except the top-mounted specimens, were placed at the bottom of the formwork as shown in Figure 9. The top-mounted specimens were pushed into the concrete after the forms were filled.

There were twelve Type II specimens. The main purpose of these Type II specimens was to determine the effect of

corner distance on the failure capacity. Direct shear was applied as in Type I but specimens were placed close to a corner as shown in Figure 6. Four Type III specimens were prepared and tested in this study. The load consisted of shear and torsion (Figure 6).

2.2.2 Concrete Slabs

Seven concrete slabs were cast for the project. All slabs were cast using commercial ready-mixed, normal-weight concrete. Three 4-in. slabs, three 8-in. slabs, and one 12-in. slab were cast. With the exception of one 8-in. slab, all the slabs were cast with bottom-mounted specimens. The mix proportions by weight of cement, flyash, fine aggregate, and coarse aggregate were 1.0:0.15:2.69:3.62. Type I cement and class C flyash were used. The coarse aggregate consisted of crushed limestone with a nominal maximum size of 1-1/2 in. Concrete properties are summarized in Table II. The concrete slabs were moist cured for seven days and then the formwork was stripped to allow for air cure.

Formwork was fabricated using dimension lumber. 4, 8, and 12-in. deep forms were made using 2-in. thick lumber. All slabs were 5 ft. x 5 ft. squares (Figure 9). 3/8-in. thick plywood strips were used on the edges of the boards so that the plates and the concrete would be flushed. Four Grade 60, No. 5 bars were cast into the middle of the slabs

so that the slabs could be handled safely during the testing. One PVC pipe, 3-in. in diameter, was cut to the slab height and inserted in the middle of the slab as shown in Figure 10. This provided a hole for a 2-in. threaded rod which was used to hold down the slab during testing.

Standard 6 in. x 12 in. test cylinders were cast and cured adjacent to the slabs. These cylinders were tested for compression strength at the end of 3 days and 7 days. The split tensile strength and compressive strength of the cylinders were obtained at the end of 21 days, when the specimens were tested.

2.2.3 Hairpin Reinforcement

Hairpin reinforcement was tack welded to the studs on specimens 1B, 2B, 2C, and 4B (Table III). Hairpins consisted of Grade 60, No. 4 bars, bent to follow the outer dimensions of the stud group (Figure 8). Based on the recommendation by ACI Committee 408 (18), an embedment of 15 in. was used to ensure development of the yield strength of the steel. The actual yield strength of the hairpin reinforcement was 54 ksi.

2.3 Test Apparatus

The test frame is shown in Figure 11. The frame was built of wide flange sections anchored to the structural test floor. Load was applied to specimens using a 30 ton hollow-core hydraulic ram. Load was monitored using a 60 kip

load cell.

The slab was supported at locations remote from the stud groups to avoid the direct contact between the potential failure area and the floor (see Figure 11). The slab was placed on two C 8 X 13.75 channels. A piece of 3/8-in. plywood was inserted between the concrete slab and the two supporting channels as a bearing pad. The slab was bolted through the floor slab with a 2-in. threaded rod (see Figure 12). This setup permitted the rotation of the slabs for further testing without the need for disassembly.

The data acquisition system consisted of a X-Y recorder, a digital strain indicator, and a linear variable differential transformer (LVDT) with a range of \pm one inch. The X-Y recorder was connected to the strain indicator and the LVDT to measure and record the load and slip respectively for each specimen. For Type I and II specimens, the LVDT was placed on the slab in the direction of the loading to measure the slip of each base plate throughout the test. The LVDT was positioned perpendicular to the direction of loading when Type III specimens were tested.

2.4 Test Procedure

All the specimens were tested at concrete ages of 21 days. The compressive strengths of the slabs are shown in Table II. The tests were conducted with a concrete strength of approximately 6000 psi to allow comparison with the

results obtained by Cruz (17).

Except for the No. 2 slab, which had top-mounted specimens, all the slabs were turned over and tested with the steel plates on the top. The slab was bolted down firmly onto the floor slab through the hole in the middle of the slab as shown in Figure 12. The load was transmitted to the specimen by two 1/2-in. plates. These plates were allowed to rotate horizontally so that no moment would be induced in the specimen. All the stud groups were loaded gradually until failure.

2.5 Test Results

2.5.1 General

The concrete strength, order of testing, and failure load for all the specimens are listed in Table IV. Some specimens were adjacent to damaged areas caused by earlier tests. However, these damaged areas did not appear to be sufficiently large to affect the failure load of the stud groups. Specimens with prior damage are indicated in Table IV.

Generally, all the specimens, except those with hairpin reinforcement, failed in a sudden manner immediately after the initial cracks appeared on the surface of the slab. The failure loads and failure surfaces for the three specimen types are described in the following sections.

2.5.2 Type I Specimens

Three distinct failure modes were observed in the Type I specimens. All of the specimens embedded in the 12-in. slabs and some of those embedded in the 8 in. slabs failed in a semi-conical shape (see Figure 13). All the specimens failed by splitting the concrete immediately after reaching the ultimate capacity. The load-slip curves for the specimens with this failure mode are shown in Figure 14. In the early part of the loading, the load-slip curve was linear. For most of the Type I specimens, a sudden slip accompanied by a slight drop in load occurred at half the ultimate capacity. This sudden slip generally occurred in the load range of 12 to 14 Kips. The load-slip behavior became nonlinear when the deflection was about 0.02 in. Most of the specimens reached their ultimate capacity in the deflection range of 0.02 to 0.07 in.

The specimens embedded in the 4 in. slabs showed a different failure pattern, i.e., they did not fail in a semi-conical shape. Instead, the cracks propagated vertically down and radiated laterally at approximately 45 degrees to the free edge as shown in Figure 15a. The cracks sometimes propagated parallel to the free edge across the whole slab (Figure 15b). The load-slip curves obtained from specimens with these failure modes are shown in Figure 16 and 17. The load-slip curves were linear until a sudden slip occurred at around 8 to 15 kips. Specimens 1C, 1D, and 2D in Figure 17 show negative slips in the initial loading stage. This was

probably caused by rotation of the slab during loading, resulting in a positive bending in the test plate. Hairpin reinforcement increased the failure capacity of a specimen slightly and provided a stiffer connection in the early part of the loading process (see Figure 18). After the specimen reached the ultimate load, the connection became very ductile. Specimens with hairpin reinforcement took a longer time to fail after reaching the ultimate load. In addition, the specimens remained intact after severe concrete failure (see Figure 19).

2.5.3 Type II Specimens

The Type II specimens consistently exhibited considerably lower failure loads than the Type I specimens. The concrete tended to split towards the corner while maintaining a semi-conical failure pattern on the side away from the corner. The failure patterns of the Type II specimens embedded in the 12 in. and 4 in. slabs are shown in Figure 20 and 21 respectively. The load-slip curves for the Type II specimens are shown in Figure 22, 23, and 24.

2.5.4 Type III Specimens

Generally, the specimens showed a slight rotation before the initial cracks appeared in the concrete. A large crack developed at the far side of the plate and propagated away from the loading direction as shown in Figure 25. Another smaller crack propagated in the direction of loading. All

Type III specimens remained intact after the ultimate load was reached. The load-slip curves for the Type III specimens are shown in Figure 26. The testing of specimen 4D was not successful due to the excessive lateral rotation of the concrete slab when it was loaded. This specimen was then loaded with direct shear.

CHAPTER III

ANALYSIS AND DISCUSSION

3.1 General

The test results described in Chapter II are used to examine the effects of edge distance, embedment length, corner distance, group width, and slab thickness on the shear capacity of stud groups. These results are compared with the capacities calculated using the procedure recommended by the PCI Design Handbook (7). Statistical analyses of the data are used to obtain design relationships which accurately reflect the behavior of the connector groups.

3.2 Evaluation of Test Results

3.2.1 Effect of Edge Distance

Edge distance (d_e) is often regarded as the most important factor affecting the strength of shear connectors. Edge distance is generally defined as the distance between the center of a stud and the free edge in the direction of loading. However, based on the observed failure pattern for stud groups with more than one row of studs, it is more appropriate to define edge distance as the distance between the center of the rear row and the free edge in the direction

of loading (Figure 27).

An increase in the edge distance will result in an increase in the nominal shear strength of the shear connection when the strength is governed by concrete failure (Figure 28 and 29). When the embedment length and edge distance are relatively large, the nominal shear strength of the connection is limited by the strength of the steel studs.

Figure 28 illustrates the effect of edge distance on the failure loads for Type I specimens. Specimens from both 4-in. and 8-in. slabs illustrate a distinct trend: as the edge distance increases, the failure load increases.

The test data for Type II specimens are plotted in Figure 29. Data for the two different slab thicknesses (4 in. and 8 in.) are shown in Figure 29. As for Type I specimens, the data show that the failure load tends to increase as the edge distance increases.

Although the data are limited, Type III specimens also show an increase in the ultimate load when the edge distance increases (Figure 30).

3.2.2 Effect of Corner Distance

Corner distance, d_c , is defined as the distance between the corner edge of a concrete slab and the center of the closest stud (see Figure 27). Only one corner distance (2.5 in.) was used in the current study. Stud groups were placed with only one side adjacent to a free edge.

Figures 31 and 32 show that specimens located away from

the corner had higher failure loads than those located near a corner. The differences in the capacities of shear connectors with and without corner effects are clearly illustrated in Figure 32.

The effect of corner distance was further amplified when the edge distance increased (see Figure 31 and 32). Figure 31 shows that connections located near a corner show a greater increase in capacity with increasing edge distance than connections located away from a corner.

3.2.3 Effect of Embedment Length

Embedment length (l_e) is the distance measured from the underside of the base plate to the end of the shank excluding the thickness of the stud head (Figure 27). Many studies have shown that embedment length is an important factor for specimens loaded in tension, and for specimens loaded in shear away from a free edge. A minimum embedment length is required to ensure that the connectors will not fail by shear cone pullout as shown in Figure 33 (19). KSM (4) and TRW (8) propose a minimum embedment length-to-diameter ratio of 4 to ensure the full development of the stud capacity.

Figures 34 and 35 show that the ultimate loads of specimens Type I and II located near a free edge were not affected significantly by an increase in the embedment length. The figures show the comparison between the types of specimens: one with $l_e/d = 3.26$ and the other with $l_e/d = 11.26$. The effect of embedment length on the Type III

specimens are shown in Figure 36 and 37. Again, there is apparently no effect of embedment length on group capacity.

3.2.4 Effect of Stud Spacing and Group Width

The width of a stud group is the out-to-out dimension transverse to the direction of load. In general, as group width increases, the ultimate load for the stud group also increases (Figure 38 and 39). The total number of studs in the row appears to have little or no effect on group capacity. Both specimens 5A and 4E had the same total width. The ratio of the failure loads for specimen 5A (2 studs) and specimen 4E (3 studs) is 1.1, indicating that the number of studs is not an important parameter.

3.2.5 Effect of Front Row Studs

The test data obtained from Cruz's report (17) was used to evaluate the effect of the front row studs on shear capacity (see Figure 40).

Specimens 2, 3, 5, 6, 8, 9, 11, 12, 14, 15, 17, and 18 were all fabricated with the same edge distance to the back row of studs. Specimens 2, 5, 8, 11, 14, and 17 had only one row of studs, while specimens 3, 6, 9, 12, 15, and 18 had 2 rows of studs. Figure 39 shows the ratios of the shear capacities of stud groups with and without front row studs versus the number of studs per row. The figure indicates that the failure load of a group is not affected significantly by the presence of front row studs. It should

be noted that all of the above specimens displayed failure in the concrete. For connector groups with capacities governed by stud shearing, as increase in the number of studs would increase capacity.

3.2.6 Effect of Slab Thickness

Three slab thicknesses (4, 8, 12 in.) were used in this investigation. Figures 28, 29, 30, 31, 32, 38 and 41 illustrate the influence of slab thickness on the failure load.

Specimens embedded in the thinner slabs tend to have a lower shear capacity than those embedded in the thicker slabs. The lower capacity of specimens embedded in the thinner slabs is due to the truncated semi-conical failure surface (Figure 15a and 15b). Specimens embedded in the thicker slabs tend to have a full semi-conical surface (see Figure 13).

Figure 41 shows that the capacities of Type III specimens were also affected by the slab thickness. Both sets of specimens, with edge distances of 2.5 in. and 5 in., showed decreases of 21.4% and 11.5%, respectively, in shear capacity as the slab thickness decreased from 12 in. to 4 in.

3.2.7 Effect of Casting Position

Section 1.2 describes two studies conducted by Maeda, Matsui, and Hiragi (13) and Kuhn and Buckner (14) on the effect of casting position on the shear capacity of

connectors.

Two casting positions were investigated in this study: bottom-mounted and top-mounted specimens. Four specimens from each category were selected to study the effect of casting position.

Figures 42 and 43 demonstrate the effect of casting position on the failure load with respect to the type of specimen and boundary condition. Of the four sets of data, three sets showed a slightly higher failure load for bottom-mounted specimens than for top-mounted specimens. This small difference (4%) in the shear capacities is probably due to the use of properly consolidated, low slump concrete. It should be noted that very few voids were observed below the top-mounted plates.

3.2.8 Effect of Hairpin Reinforcement

Four specimens were fabricated with Grade 60 #4 mild steel reinforcing bars. Stud groups with hairpin reinforcement displayed much higher ductility than similar groups without reinforcement (Figure 44).

The ultimate loads for stud groups with hairpin reinforcement were governed by the tensile strength of the reinforcement. For two #4 bars with yield strengths of 54 Ksi, the ultimate capacity of the group should be 21.6 Kips. This compares with the ultimate capacities of 17.92 Kips, 22.68 Kips, and 15.74 Kips, for groups 2C, 1B, and 4B.

As edge distance decreases, the effect of hairpin

reinforcement on group strength becomes more significant. Stud groups located near a free edge will display an initial failure in the concrete at relatively low loads. The reinforcement, which crosses the failure surface, will continue to carry load up to its tensile capacity. Specimens 2C and 3C, 1B and 3B, and 4B and 5B were similar in geometry and edge distance (2.5, 5 and 5 in., respectively). The ratios of the capacities of the specimens with reinforcement to the capacities of the specimens without reinforcement were 1.85, 1.14, and 1.11, respectively.

3.3 Empirical Design Equations

The test data from the current investigation and from Cruz's study (17) clearly indicate that the nominal shear capacity of a headed stud group connection limited by concrete failure is directly related to the area of the failure surface. The parameters that affect the concrete failure surface are the edge distance, corner distance, lateral stud spacing, group width, and slab thickness. Other factors, such as embedment length, front row studs, and casting position, appear to have only a very small influence on the size of the failure surface (and thus, the capacity of the group).

Earlier studies indicated that the embedment length is not an important parameter affecting the shear capacity of a connection. The current investigation and Cruz's experiments (17) show that stud groups with embedment length-to-diameter

ratios of 3.26 and 11.26 perform almost identically in their shear carrying capacity. Embedment length of more than $4d$ is, therefore, not considered in the statistical evaluations.

The experimental data indicate that the front row studs may be disregarded in determining the nominal shear strength of connections controlled by concrete failure. (Note: front row studs may be important when the strength is controlled by the studs.) Whenever two or more rows of studs are used, the edge distance for the furthest row is used in the statistical analysis.

Casting position is not considered as a parameter in the statistical analysis.

The shear capacity of a connection controlled by concrete failure is assumed to be proportional to $\sqrt{f'_c}$ normal to the failure surface in the direction of load times the approximate area of the failure surface.

3.3.1 Type I Specimens

The distance between the base of the stud head and the bottom of the slab with respect to edge distance determines whether a slab is "thick" or "thin". When this distance $t - 4d$ is greater than $\sqrt{2}d_e$ ("thick" slabs), the failure surface tends to propagate 45 degrees from the plane of loading as shown in Figure 13. The area of the failure surface is obtained from the shaded area (Figure 45) and projected at 45 degree.

$$\text{Area} = \sqrt{2}d_e[d_e + S_x(n-1)] \quad (3.1)$$

where:

t = slab thickness (in.)

d = diameter of stud (in. ²)

d_e = edge distance (in.)

S_x = lateral stud spacing (in.)

n = number of studs in the back row.

When $t - 4d$ is less than or equal to $\sqrt{2}d_e$ ("thin" slabs), the failure surface develops to the nearest edge by propagating vertically down, as shown in Figure 15a and 15b. The area of the failure surface for the "thin" slabs is approximated as (see Figure 46):

$$\text{Area} = 2d_e t + S_x(n-1)t \quad (3.2)$$

Based on a regression analysis using the test data obtained in this investigation and Cruz's investigation (17), the nominal shear strength of a connector is given by:

For Type I specimen embedded in "thick" slabs,

$$(t - 4d) > \sqrt{2} d_e \quad (3.3)$$

$$\text{Area} = (\sqrt{2})d_e[d_e + S_x(n-1)]$$

$$V_n = 18.3716(\sqrt{f'_c})\{\sqrt{2}d_e[d_e + S_x(n-1)]^{0.6035}\} \quad (3.4)$$

where:

V_n = nominal shear capacity (lb.)

f'_c = concrete compressive strength (psi);

For Type I specimens embedded in "thin" slabs,

$$(t - 4d) \leq \sqrt{2} d_e \quad (3.5)$$

$$\text{Area} = 2d_e t + S_x(n-1)t$$

$$V_n = 6.4098(\sqrt{f'_c})[2d_e t + S_x(n-1)t]^{0.7673} \quad (3.6)$$

3.3.2 Type II Specimens

The failure pattern for stud groups located near a corner was very distinct. As a result, accurate assumptions could be made to establish the limit of corner effects. Generally, specimens positioned away from the corner had top-surface cracks which propagated at approximately 45 degrees to the direction of loading, while specimens located near a corner had a top-surface crack which propagated normal to the loading direction directly to the corner (Figure 20 and 21). A study of the failure pattern indicated that the cracks tend to develop to the side of the slab when $\sqrt{2}d_e \geq d_c$. Figure 47 shows the approximate area of failure surface for Type II, "thick" slabs and the equation is given by:

$$\text{Area} = (\sqrt{2})d_e[\frac{1}{2}d_e + S_x(n-1) + d_c] \quad (3.7)$$

where:

d_c = corner distance (in.)

The shaded area in Figure 48 shows the area of failure surface for Type II, "thin" slabs. The area is approximated as:

$$\text{Area} = d_e t + d_c t + S_x(n-1)t \quad (3.8)$$

Based on regression analyses, the following equations on the nominal shear capacity are obtained:

For Type II specimens embedded in "thick" slabs,

$$(t - 4d) > \sqrt{2} d_e$$

$$\text{Area} = (\sqrt{2})d_e[\frac{1}{2}d_e + S_x(n-1) + d_c]$$

$$V_{nc} = 5.930(\sqrt{f'_c})\{(\sqrt{2}d_e[\frac{1}{2}d_e + S_x(n-1) + d_c])^{0.7997}\} \quad (3.9)$$

where:

V_{nc} = nominal shear capacity with corner effect (lb.);

For Type II specimens embedded in "thin" slabs,

$$(t - 4d) \leq \sqrt{2} d_e$$

$$\text{Area} = d_e t + d_c t + S_x(n-1)t$$

$$V_{nc} = 6.2129(\sqrt{f'_c})[d_e t + d_c t + S_x(n-1)t]^{0.7002}. \quad (3.10)$$

Figure 49 is plotted using eq. 3.4, 3.5, 3.9, 3.10 versus test data obtained from current study and Cruz's experiment (17).

Eq. (3.4, 3.6, 3.9, and 3.10) were simplified for design purposes by setting the exponent of the area of the failure surface to 3/4. The new coefficients for each equations were obtained as follow:

For Type I specimens embedded in "thick" slabs:

$$V_n = 7(\sqrt{f'_c})\{\sqrt{2}d_e[d_e + S_x(n-1)]^{3/4}\} \quad (3.11)$$

For Type I specimens embedded in "thin" slabs:

$$V_n = 11(\sqrt{f'_c})[2d_e t + S_x(n-1)t]^{3/4} \quad (3.12)$$

For Type II specimens embedded in "thick" slabs:

$$V_{nc} = 5(\sqrt{f'_c})\{\sqrt{2}d_e[\frac{1}{2}d_e + S_x(n-1) + d_c]^{3/4}\} \quad (3.13)$$

For Type II specimens embedded in "thin" slabs:

$$V_{nc} = 7(\sqrt{f'_c})[d_e t + d_c t + S_x(n-1)t]^{3/4} \quad (3.14)$$

The above equations also apply to single stud connections loaded in shear by setting $S_x(n-1) = d$. Figure 50 compares the failure loads with the predicted capacities for all of the Type I and II specimens. The predicted capacities are based on Eq. 3.11, 3.12, 3.13, and 3.14.

Figure 51 gives a comparison between the predicted capacity for Type I specimens based on Eq. 3.11 and 3.12 and

the predicted capacity obtained using the PCI equations (see Appendix E).

CHAPTER IV

SUMMARY AND CONCLUSIONS

4.1 Summary

The purpose of this study was to investigate the effects of edge distance, corner distance, embedment length, lateral stud spacing and group width, front row studs, slab thickness, casting position, and hairpin reinforcement on the capacity and failure behavior of headed stud groups embedded in normal-weight concrete. Seven slabs were cast with a total of thirty-three test specimens. 1/2-in. diameter studs were used throughout the test. The slabs were cast in three thicknesses (4, 8, and 12-in.). The edge distances were 2.5, 5, and 7.5 in.. The test data were combined with Cruz's data (17) to study the effect of each of these variables.

Empirical equations based on statistical analyses for the shear capacity of stud groups embedded in normal weight concrete are established. Capacities of connections calculated using the procedure suggested by the PCI Design Handbook (7) are compared with the test results.

4.2 Conclusions

The following conclusions are based on the test results and analyses described in this report:

- 1) Edge distance is the most important factor governing the shear capacity of a stud group connection. The capacity of shear connections increases as the edge distance increases.
- 2) The capacity of shear connections increases as the corner distance increases. The effect of corner distance appears to be effective when $d_c < \sqrt{2}d_e$.
- 3) The capacity of a stud group is also affected by the width of the stud group. The number of studs in the back row does not affect the strength of the group.
- 4) The contribution of the front row studs on the ultimate shear capacity of a stud group located near a free edge is insignificant.
- 5) "Thick" slabs tend to exhibit semi-conical failure surfaces. "Thin" slabs tend to exhibit vertical failure surfaces. Therefore, the shear capacity of a connection embedded in a "thin" slab is lower than the capacity of a connection embedded in a "thick" slab.
- 6) Shear capacity is not affected by the casting position when low slump, properly consolidated concrete is used.
- 7) Hairpin reinforcement increases shear capacity for specimens with a small edge distance. The effect is not significant for specimens with large edge distance. In either case, hairpin reinforcement

provides a more ductile failure pattern.

4.3 Future Work

The empirical equations derived in the current study are based on data from tests of slabs fabricated with normal weight, 6000 psi concrete. Different concrete strengths, ranging between 4000 and 8000 psi, should be investigated. The behavior of headed stud groups in lightweight concrete should also be investigated.

The current investigation shows that corner distance is a significant parameter affecting the nominal shear capacity of a stud group. This study was, however, restricted to only one corner distance. Different corner distances should be incorporated in future research. In addition, investigation of specimens with a corner on each side of a stud group should be included in future studies.

Larger stud diameters, such as 5/8 and 3/4 in., should be used in future tests.

More data are needed to study the effects of lateral stud spacing on shear capacity. Future investigations should include 2, 4, 6, and 8-in. lateral stud spacing with large edge distances.

The effect of embedment length requires further investigation.

The effect of slab thickness on connector strength requires further investigation. Slabs with thickness of 16-in. or more should be evaluated.

Combined shear and torsion, and combined shear and tension should be evaluated further.

A rational analysis technique, based on nonlinear fracture mechanics, should be developed.

A SELECTED BIBLIOGRAPHY

1. Bode, H., Roik, K., "Headed Studs - Embedded in Concrete and Loaded in Tension," Anchorage to Concrete, Special Publication 103-4, pp. 61-88.
2. Hawkins, N., "Strength in Shear and Tension of Cast-in-Place Anchor Bolts," Anchorage to Concrete, Special Publication 103-12, pp. 233-255.
3. PCI Manual on Design of Connections for Precast Prestressed Concrete, Prestressed Concrete Institute, 1973.
4. KSM Structural Engineering Aspects of Headed Concrete Anchors and Deformed Bar Anchors in the Concrete Construction Industry, KSM Fastening Systems Division, Omark Industries, 1974.
5. Shaikh, A. F., Yi, W., "In-Place Strength of Welded Headed Studs," PCI Journal, Vol. 30, No. 2, March-April 1985, pp. 56-81.
6. ACI Committee 349, "Proposed Addition to: Code Requirements for Nuclear Safety Related Structures (ACI 349-76)," and "Addition to Commentary on Code Requirements for Nuclear Safety Related Structures (ACI 349-76)," ACI Journal, Proceedings v. 75, No. 8, Aug. 1978, pp. 329-347.
7. PCI Design Handbook - Precast and Prestress Concrete, 2nd Edition, Prestress Concrete Institute, Chicago, 1978.
8. "Embedded Properties of Headed Studs - Design Data 10," TRW Nelson Division.
9. PCI Manual for Structural Design of Architectural Precast Concrete, Prestress Concrete Institute, Chicago, Illinois, 1977.
10. "Concrete Anchorages," TVA Civil Design Standard, No. DS-C6.1, Tennessee Valley Authority, Knoxville, 1975.

11. Ollgaard, J. G., Slutter, R. G., Fisher, J. W., "Shear Strength of Stud Connectors in Light Weight and Normal-Weight Concrete," Engineering Journal of the American Institute of Steel Construction, Vol. 8, No. 2., April 1971, pp 55-64.
12. Cannon, R. W., Burdette, E. G., and Funk, R. R., "Anchorage to Concrete," Report No. CEB 75-32, Tennessee Valley Authority, Knoxville, Dec. 1975.
13. Maeda, Y., Matsui, S., Hiragi, H., "Effects of Concrete-Placing Direction on Static and Fatigue Strengths of Stud Shear Connectors," Technology Reports of the Osaka University, Vol. 33, No. 1733, October 1983, pp. 397-406.
14. Kuhn, J. M., Buckner, C. D., "Effect of Concrete Placement on Shear Strength of Headed Studs," Journal of Structural Engineering, Vol. 112, No. 8, August 1986.
15. Klingner, R. E., Mendonca, J. A., Malik, J. B., "Effect of Reinforcing Details on the Shear Resistance of Anchor Bolts Under Reversed Cyclic Loading," ACI Journal, Vol. 79, No. 1, January-February 1982, pp. 3-12.
16. McMackin, P. J., Slutter, R. G., Fisher, J. W., "Headed Steel Anchor under Combined Loading," AISC Engineering Journal, Vol. 10, No. 2, Second Quarter 1973, pp. 43-52.
17. Cruz, R. D., "Effect of Edge Distance on Stud Groups Loaded in Shear and Torsion," Civil Engineering Reports, Oklahoma State University, December 1986.
18. ACI Committee 408, "Suggested Development, Splice, and Standard Hook Provisions for Deformed Bars in Tension," ACI, Detroit, 1979.
19. Klingner, R. E., Mendonca, J. A., "Shear Capacity of Short Anchor Bolts and Welded Studs: A Literature Review," ACI Journal, September-October 1982, pp. 339-349.

APPENDIX A

TABLES

TABLE I
STUD SPECIFICATION

Stud Type	Nelson Stud 1/2" X 2-1/8" H4L
Grade	C - 1015
Heat No.	L 21873
Carbon	0.14
Manganese	0.58
Phosphorus	0.008
Sulfur	0.010
Ultimate Strength*	64.6 Ksi
Yield Strength*	55.2 Ksi
% Reduction of Area	68.9
% Elongation	43.4

* Based on original cross section

TABLE II
PROPERTIES OF CONCRETE

Phase	I	II
Slump (in.)	2.5	2.0
Compressive Strength (psi)	6020	5840
Tensile Strength (psi)	470	600
Modulus of Elasticity (psi)	4.06×10^7	4.14×10^7
Dry Unit Weight (lb. /ft. ³)	149.5	150.7

TABLE III
SPECIMENS SPECIFICATION

Specimen Number	Stud Pattern	d (in.)	le (in.)	Number of Studs		Sx (in.)	Sy (in.)	t (in.)	de (in.)	dc (in.)	Casting Position	Specimen Type	Hairpin Y-Yes N-No
				Back Row	Front Row								
1 A	A	1/2	1.63	2	0	6	0	8	5	2.5	BOTTOM	II	N
1 B	A	"	"	2	0	6	0	8	5	20	"	I	Y
1 C	I	"	"	2	1	6	5	8	7.5	20	"	I	N
1 D	H	"	"	2	1	6	2.5	8	7.5	20	"	I	N
1 E	C	"	"	2	1	6	2.5	8	5	2.5	"	II	N
2 A	A	"	"	2	0	6	0	8	5	2.5	TOP	II	N
2 B	A	"	"	2	0	6	0	8	5	20	"	I	Y
2 C	J	"	"	2	0	6	0	8	2.5	20	"	I	Y
2 D	H	"	"	2	1	6	2.5	8	7.5	20	"	I	N
2 E	H	"	"	2	1	6	2.5	8	7.5	2.5	"	II	N
3 A	J	"	"	2	0	6	0	8	2.5	2.5	BOTTOM	II	N
3 B	A	"	"	2	0	6	0	8	5	20	"	I	N
3 C	J	"	"	2	0	6	0	8	2.5	20	"	I	N
3 D	C	"	"	2	1	6	2.5	8	5	20	"	I	N
3 E	G	"	"	2	0	6	0	8	7.5	2.5	"	II	N
4 A	D	"	"	2	0	4	0	4	5	2.5	"	II	N
4 B	A	"	"	2	0	6	0	4	5	20	"	I	Y
4 C	J	"	"	2	0	6	0	4	2.5	20	"	I	N
4 D	H	"	"	2	1	6	2.5	4	7.5	20	"	III	N
4 E	B	"	"	3	0	3	0	4	5	2.5	"	II	N
5 A	A	"	"	2	0	6	0	4	5	2.5	"	II	N
5 B	A	"	"	2	0	6	0	4	5	20	"	I	N
5 C	K	"	"	3	0	2	0	4	2.5	20	"	III	N
5 D	H	"	"	2	1	6	2.5	4	7.5	20	"	I	N
5 E	J	"	"	2	0	6	0	4	2.5	2.5	"	II	N
6 A	A	"	"	2	0	6	0	12	5	2.5	"	II	N
6 B	E	"	"	3	0	2	0	12	5	20	"	I	N
6 C	K	"	"	3	0	2	0	12	2.5	20	"	I	N
6 D	A	"	"	2	0	6	0	12	5	20	"	I	N
6 E	D	"	"	2	0	4	0	12	5	2.5	"	II	N
7 A	F	"	"	2	2	4	2.5	4	5	20	"	III	N
7 B	L	"	"	2	0	4	0	4	2.5	20	"	III	N
7 C	J	"	"	2	0	6	0	4	2.5	20	"	III	N

TABLE IV
TEST RESULTS

Specimen Number	Concrete Strength f'c(ksi)	Order of Testing	Ultimate Load (kips)	Previous Damage
1 A	6.02	6	11.38	No
1 B	6.02	10	22.68	Yes
1 C	6.02	8	24.47	No
1 D	6.02	9	24.39	Yes
1 E	6.02	7	12.08	No
2 A	6.02	12	10.75	No
2 B	6.02	13	21.51	No
2 C	6.02	15	17.92	No
2 D	6.02	14	26.96	No
2 E	6.02	11	14.03	No
3 A	5.84	24	7.09	No
3 B	5.84	28	19.71	No
3 C	5.84	26	9.58	No
3 D	5.84	27	19.33	No
3 E	5.84	25	16.05	No
4 A	6.02	2	7.64	No
4 B	6.02	3	15.74	No
4 C	6.02	4	7.45	No
4 D	6.02	5	12.19	Yes
4 E	6.02	1	7.79	No
5 A	5.84	20	8.57	No
5 B	5.84	23	14.03	Yes
5 C	5.84	19	8.42	No
5 D	5.84	22	17.58	Yes
5 E	5.84	21	5.92	No
6 A	5.84	30	13.68	No
6 B	5.84	32	16.44	No
6 C	5.84	31	8.42	No
6 D	5.84	33	20.73	No
6 E	5.84	29	12.94	No
7 A	5.84	16	15.04	No
7 B	5.84	18	9.35	No
7 C	5.84	17	9.43	No

* All specimens failed in concrete.

APPENDIX B

FIGURES

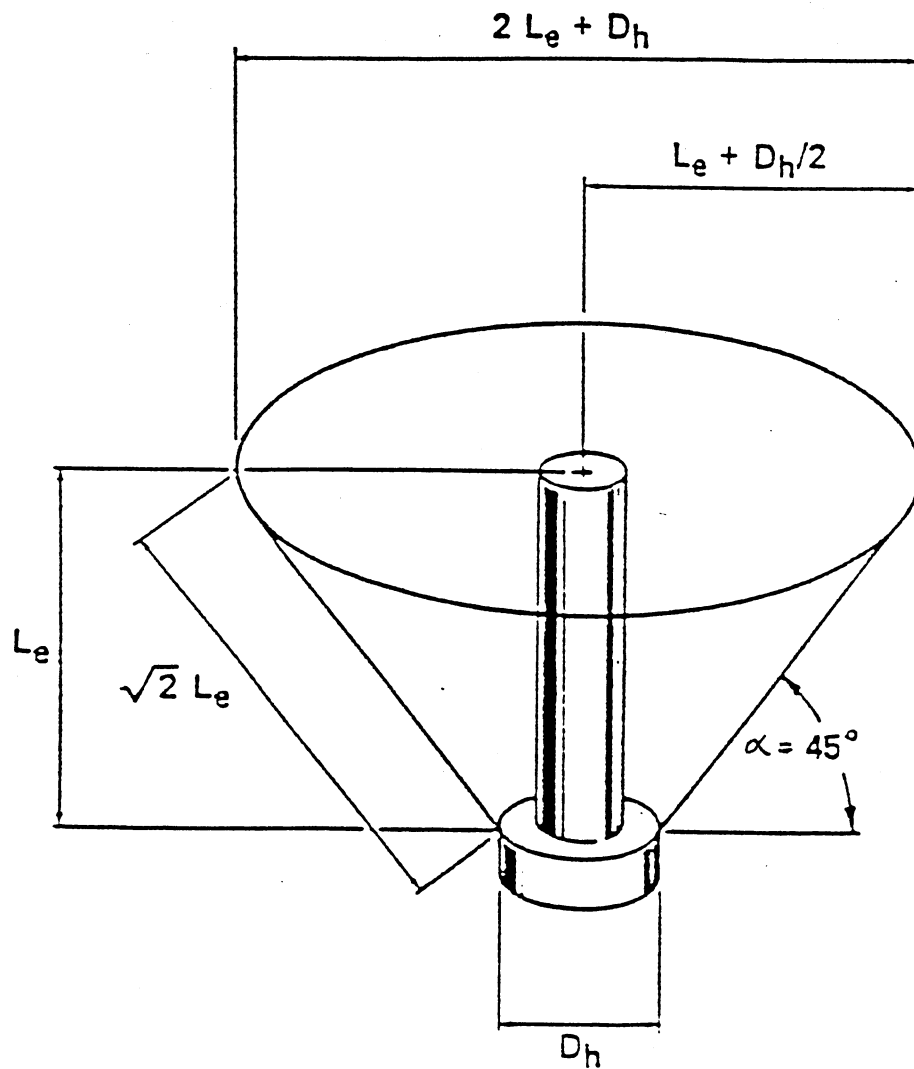


Figure 1 Pullout Failure for Concrete Loaded in Tension (8)

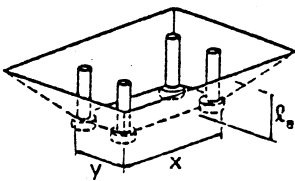
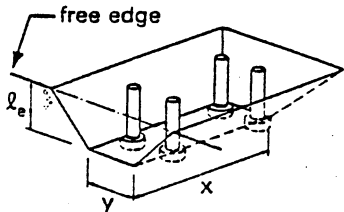
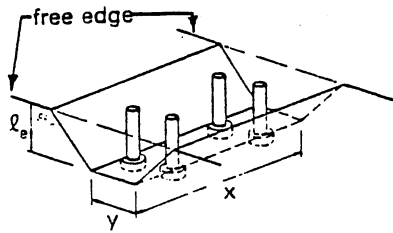
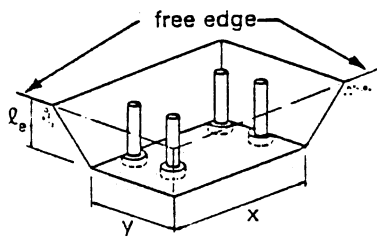
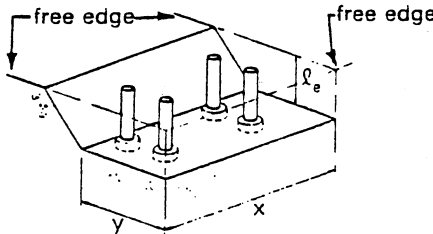
<p>Note: For each case, use lesser of P_{c1} or P_{c2}</p>	
	<p>Case 1: Not near a free edge</p> $P_{c1} = 4\lambda \sqrt{f'_c} [xy + 2\ell_e (x + y) + 4\ell_e^2]$ $P_{c2} = 4\lambda \sqrt{f'_c} [2h(x + y + 4\ell_e - 4h) + 4h^2]$ <p>h = member thickness (see Fig 6.5.4)</p>
	<p>Case 2: Near a free edge on one side</p> $P_{c1} = 4\lambda \sqrt{f'_c} [xy + \ell_e (2x + y) + 2\ell_e^2]$ $P_{c2} = 4\lambda \sqrt{f'_c} [h(2x + y + 6\ell_e - 6h) + 2h^2]$
	<p>Case 3: Near a free edge on 2 opposite sides</p> $P_{c1} = 4\lambda \sqrt{f'_c} (xy + 2\ell_e x)$ $P_{c2} = 4\lambda \sqrt{f'_c} 2h(x + 2\ell_e - 2h)$
	<p>Case 4: Near a free edge on 2 adjacent sides</p> $P_{c1} = 4\lambda \sqrt{f'_c} [xy + \ell_e (x + y) + \ell_e^2]$ $P_{c2} = 4\lambda \sqrt{f'_c} [h(x + y + 4\ell_e - 4h) + h^2]$
	<p>Case 5: Near a free edge on 3 sides</p> $P_{c1} = 4\lambda \sqrt{f'_c} (xy + \ell_e x)$ $P_{c2} = 4\lambda \sqrt{f'_c} h(x + 2\ell_e - 2h)$

Figure 2 Pullout Surface Areas for Stud Groups (7)

	<p>Case 1: Not near a free edge*</p> <table border="1"> <tr> <td>$h \geq (z + 2l_e)/2$</td><td>$P_{nc} = 4\lambda\sqrt{f'_c} (x+2l_e)(y+2l_e)$</td></tr> <tr> <td>$h < (z + 2l_e)/2$</td><td>$P_{nc} = 4\lambda\sqrt{f'_c} ((x+2l_e)(y+2l_e) - A_R^{\dagger})$</td></tr> </table>	$h \geq (z + 2l_e)/2$	$P_{nc} = 4\lambda\sqrt{f'_c} (x+2l_e)(y+2l_e)$	$h < (z + 2l_e)/2$	$P_{nc} = 4\lambda\sqrt{f'_c} ((x+2l_e)(y+2l_e) - A_R^{\dagger})$
$h \geq (z + 2l_e)/2$	$P_{nc} = 4\lambda\sqrt{f'_c} (x+2l_e)(y+2l_e)$				
$h < (z + 2l_e)/2$	$P_{nc} = 4\lambda\sqrt{f'_c} ((x+2l_e)(y+2l_e) - A_R^{\dagger})$				
	<p>Case 2: Free edge on one side</p> <table border="1"> <tr> <td>$h \geq (z + 2l_e)/2$</td><td>$P_{nc} = 4\lambda\sqrt{f'_c} (x+l_e+d_e)(y+2l_e)$</td></tr> <tr> <td>$h < (z + 2l_e)/2$</td><td>$P_{nc} = 4\lambda\sqrt{f'_c} ((x+l_e+d_e)(y+2l_e) - A_R^{\dagger})$</td></tr> </table>	$h \geq (z + 2l_e)/2$	$P_{nc} = 4\lambda\sqrt{f'_c} (x+l_e+d_e)(y+2l_e)$	$h < (z + 2l_e)/2$	$P_{nc} = 4\lambda\sqrt{f'_c} ((x+l_e+d_e)(y+2l_e) - A_R^{\dagger})$
$h \geq (z + 2l_e)/2$	$P_{nc} = 4\lambda\sqrt{f'_c} (x+l_e+d_e)(y+2l_e)$				
$h < (z + 2l_e)/2$	$P_{nc} = 4\lambda\sqrt{f'_c} ((x+l_e+d_e)(y+2l_e) - A_R^{\dagger})$				
	<p>Case 3: Free edges on 2 opposite sides</p> <table border="1"> <tr> <td>$h \geq (z + 2l_e)/2$</td><td>$P_{nc} = 4\lambda\sqrt{f'_c} (x+d_{e1}+d_{e2})(y+2l_e)$</td></tr> <tr> <td>$h < (z + 2l_e)/2$</td><td>$P_{nc} = 4\lambda\sqrt{f'_c} ((x+d_{e1}+d_{e2})(y+2l_e) - A_R^{\dagger})$</td></tr> </table>	$h \geq (z + 2l_e)/2$	$P_{nc} = 4\lambda\sqrt{f'_c} (x+d_{e1}+d_{e2})(y+2l_e)$	$h < (z + 2l_e)/2$	$P_{nc} = 4\lambda\sqrt{f'_c} ((x+d_{e1}+d_{e2})(y+2l_e) - A_R^{\dagger})$
$h \geq (z + 2l_e)/2$	$P_{nc} = 4\lambda\sqrt{f'_c} (x+d_{e1}+d_{e2})(y+2l_e)$				
$h < (z + 2l_e)/2$	$P_{nc} = 4\lambda\sqrt{f'_c} ((x+d_{e1}+d_{e2})(y+2l_e) - A_R^{\dagger})$				
	<p>Case 4: Free edges on 2 adjacent sides</p> <table border="1"> <tr> <td>$h \geq (z + 2l_e)/2$</td><td>$P_{nc} = 4\lambda\sqrt{f'_c} (x+l_e+d_{e1})(y+l_e+d_{e2})$</td></tr> <tr> <td>$h < (z + 2l_e)/2$</td><td>$P_{nc} = 4\lambda\sqrt{f'_c} ((x+l_e+d_{e1})(y+l_e+d_{e2}) - A_R^{\dagger})$</td></tr> </table>	$h \geq (z + 2l_e)/2$	$P_{nc} = 4\lambda\sqrt{f'_c} (x+l_e+d_{e1})(y+l_e+d_{e2})$	$h < (z + 2l_e)/2$	$P_{nc} = 4\lambda\sqrt{f'_c} ((x+l_e+d_{e1})(y+l_e+d_{e2}) - A_R^{\dagger})$
$h \geq (z + 2l_e)/2$	$P_{nc} = 4\lambda\sqrt{f'_c} (x+l_e+d_{e1})(y+l_e+d_{e2})$				
$h < (z + 2l_e)/2$	$P_{nc} = 4\lambda\sqrt{f'_c} ((x+l_e+d_{e1})(y+l_e+d_{e2}) - A_R^{\dagger})$				
	<p>Case 5: Free edges on 3 sides</p> <table border="1"> <tr> <td>$h \geq (z + 2l_e)/2$</td><td>$P_{nc} = 4\lambda\sqrt{f'_c} (x+d_{e1}+d_{e2})(y+l_e+d_{e3})$</td></tr> <tr> <td>$h < (z + 2l_e)/2$</td><td>$P_{nc} = 4\lambda\sqrt{f'_c} ((x+d_{e1}+d_{e2})(y+l_e+d_{e3}) - A_R^{\dagger})$</td></tr> </table>	$h \geq (z + 2l_e)/2$	$P_{nc} = 4\lambda\sqrt{f'_c} (x+d_{e1}+d_{e2})(y+l_e+d_{e3})$	$h < (z + 2l_e)/2$	$P_{nc} = 4\lambda\sqrt{f'_c} ((x+d_{e1}+d_{e2})(y+l_e+d_{e3}) - A_R^{\dagger})$
$h \geq (z + 2l_e)/2$	$P_{nc} = 4\lambda\sqrt{f'_c} (x+d_{e1}+d_{e2})(y+l_e+d_{e3})$				
$h < (z + 2l_e)/2$	$P_{nc} = 4\lambda\sqrt{f'_c} ((x+d_{e1}+d_{e2})(y+l_e+d_{e3}) - A_R^{\dagger})$				
	<p>Case 6: Free edges on 4 sides</p> <table border="1"> <tr> <td>$h \geq (z + 2l_e)/2$</td><td>$P_{nc} = 4\lambda\sqrt{f'_c} (x+d_{e1}+d_{e2})(y+d_{e3}+d_{e4})$</td></tr> <tr> <td>$h < (z + 2l_e)/2$</td><td>$P_{nc} = 4\lambda\sqrt{f'_c} ((x+d_{e1}+d_{e2})(y+d_{e3}+d_{e4}) - A_R^{\dagger})$</td></tr> </table>	$h \geq (z + 2l_e)/2$	$P_{nc} = 4\lambda\sqrt{f'_c} (x+d_{e1}+d_{e2})(y+d_{e3}+d_{e4})$	$h < (z + 2l_e)/2$	$P_{nc} = 4\lambda\sqrt{f'_c} ((x+d_{e1}+d_{e2})(y+d_{e3}+d_{e4}) - A_R^{\dagger})$
$h \geq (z + 2l_e)/2$	$P_{nc} = 4\lambda\sqrt{f'_c} (x+d_{e1}+d_{e2})(y+d_{e3}+d_{e4})$				
$h < (z + 2l_e)/2$	$P_{nc} = 4\lambda\sqrt{f'_c} ((x+d_{e1}+d_{e2})(y+d_{e3}+d_{e4}) - A_R^{\dagger})$				

*Near a free edge implies $d_e < l_e$.

$^{\dagger}z$ is equal to the lesser of the "x" and "y" values.

$^{\ddagger}A_R = (x + 2l_e - 2h)(y + 2l_e - 2h)$.

Note: The nominal tension strength (P_{nc}) values given in the table are obtained by using stress levels of $(4/\sqrt{2})\sqrt{f'_c}$ on the sloping sides area and $4\sqrt{f'_c}$ on the base area of the failure surface, respectively.

Figure 3 Stud Groups in Tension (5)

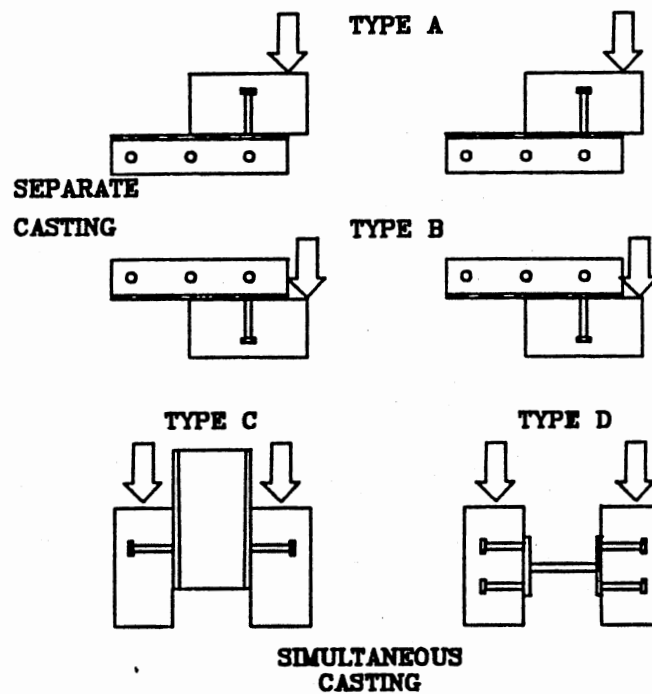


Figure 4 Concrete Placement Direction (13)

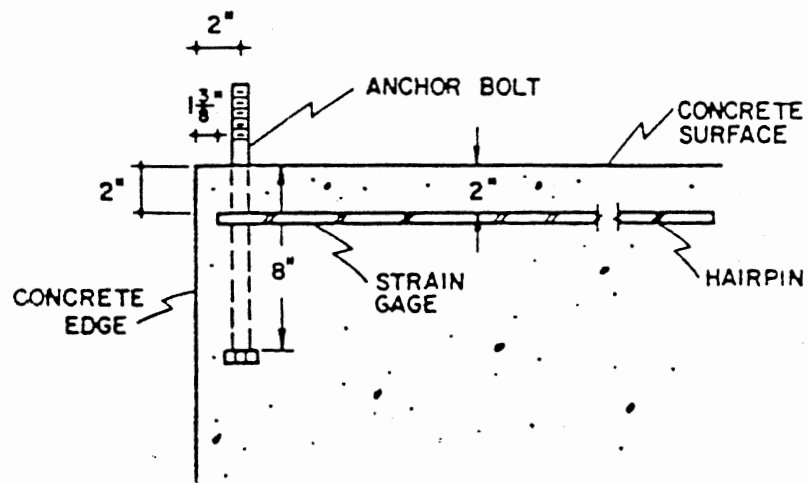


Figure 5 Suggested Method of Placement for Hairpin Reinforcement (15)

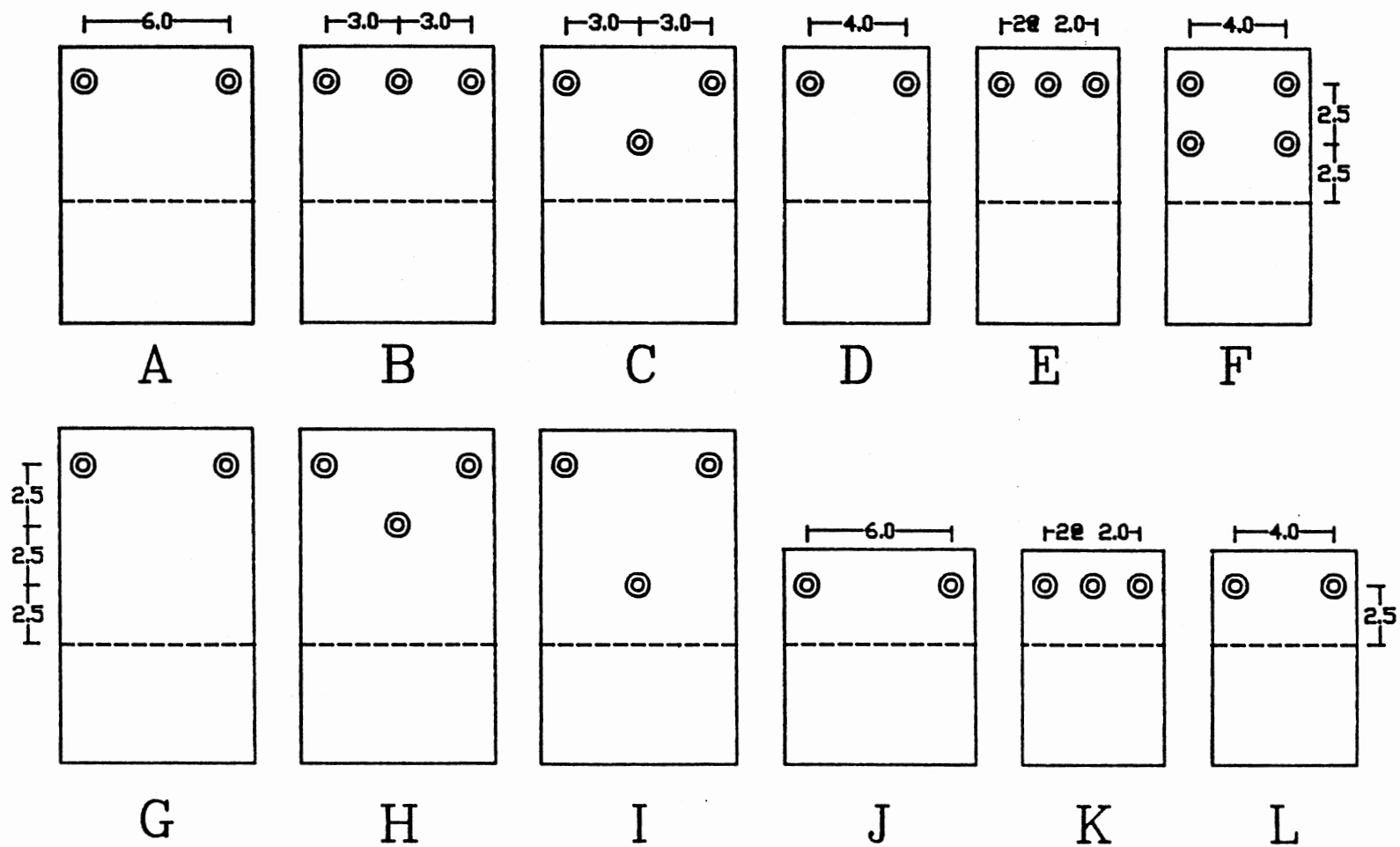


Figure 7 Configurations of Stud Groups

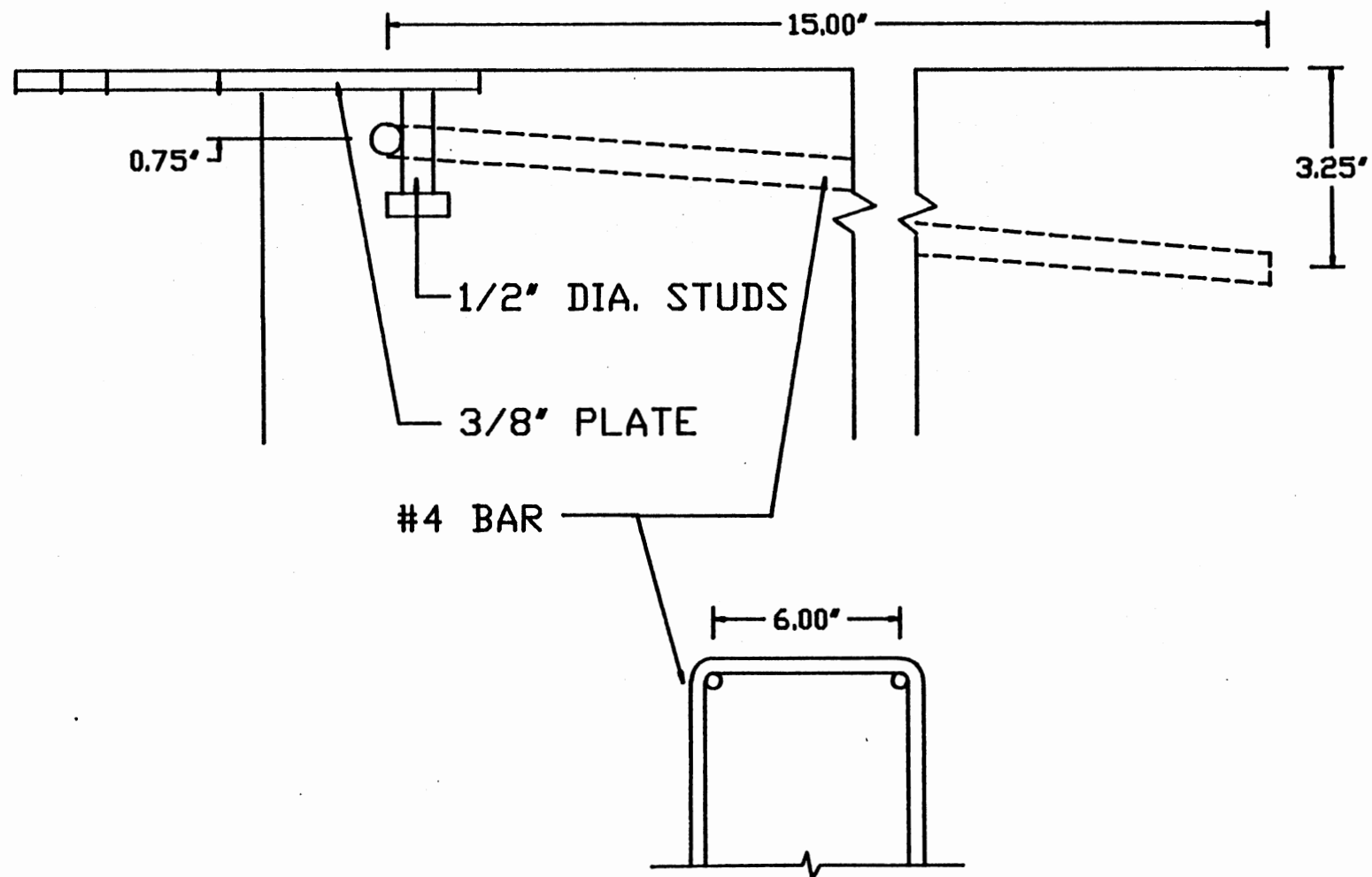


Figure 8 Details of Specimen with Hairpin Reinforcement

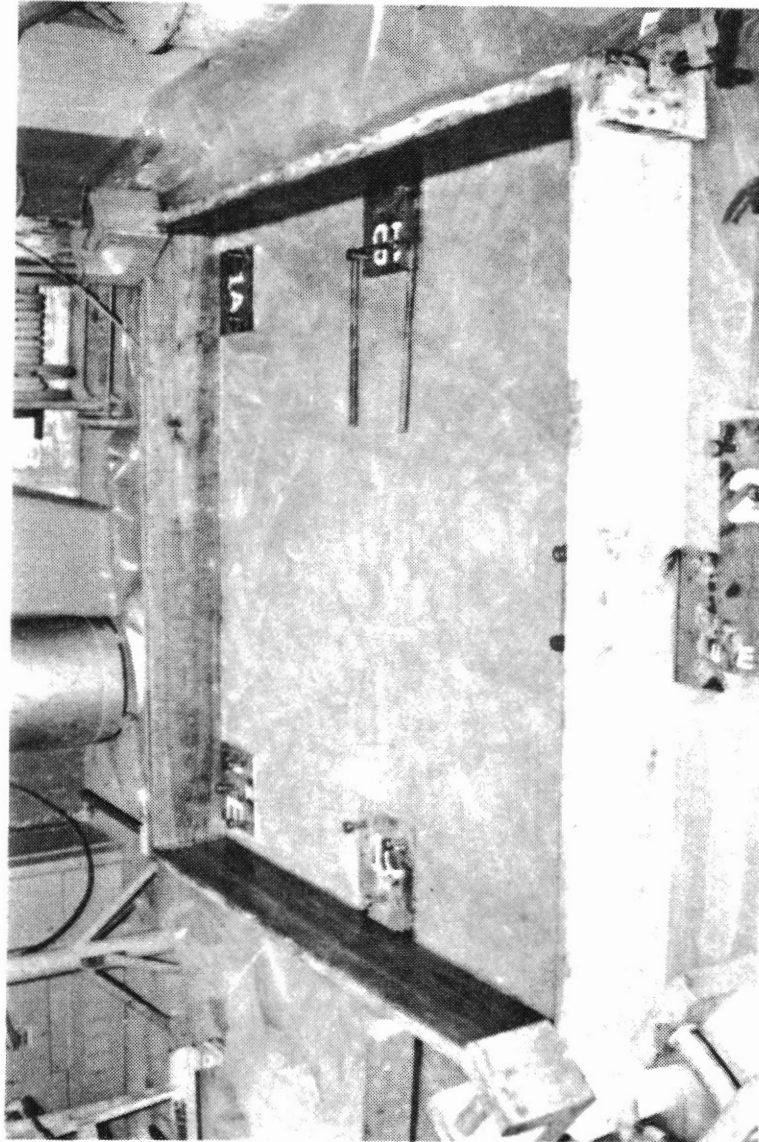


Figure 9 Position of Stud Groups



Figure 10 Position of PVC Pipe and Concrete Inserts

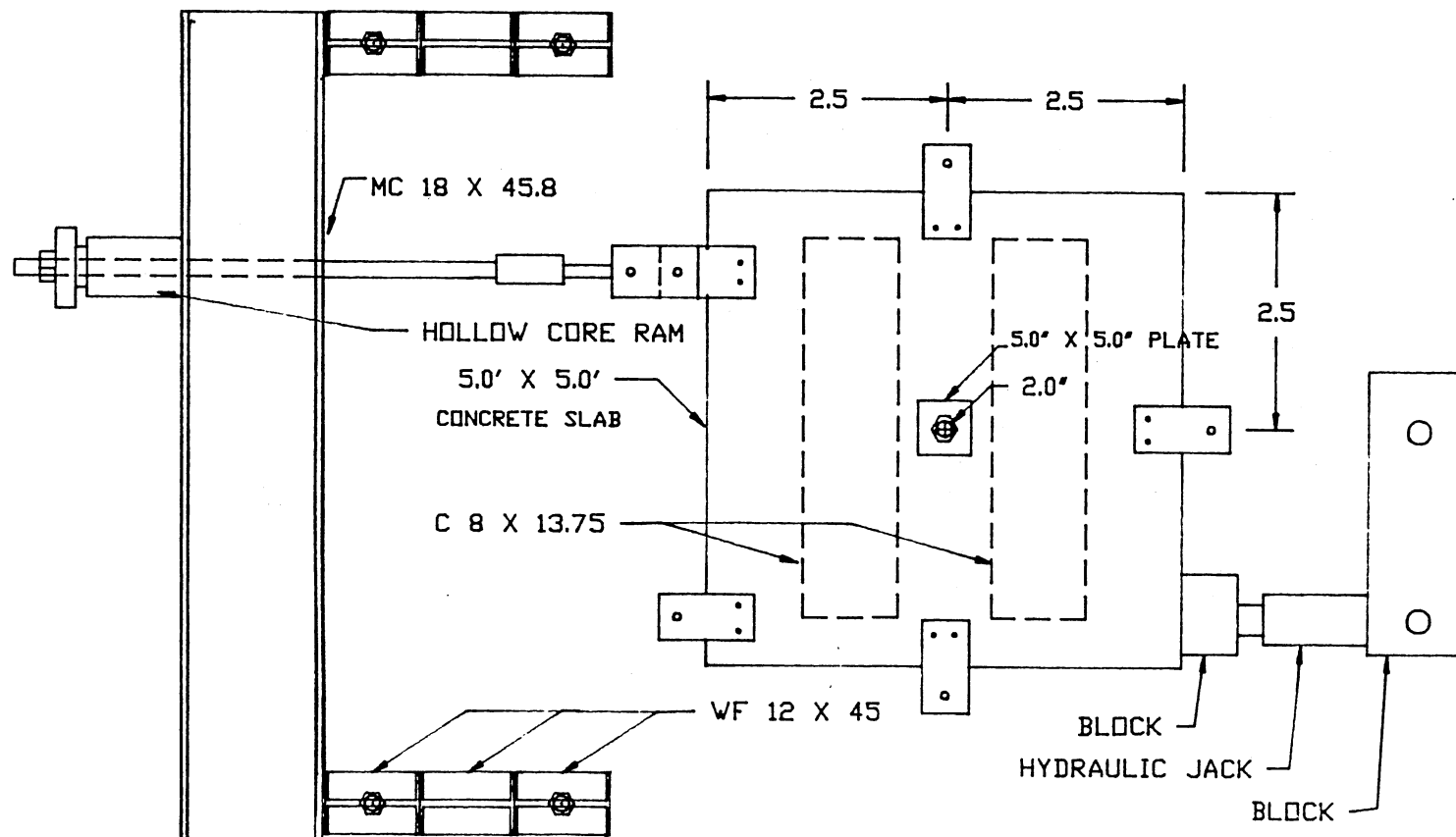


Figure 11 Test Apparatus (Plan)

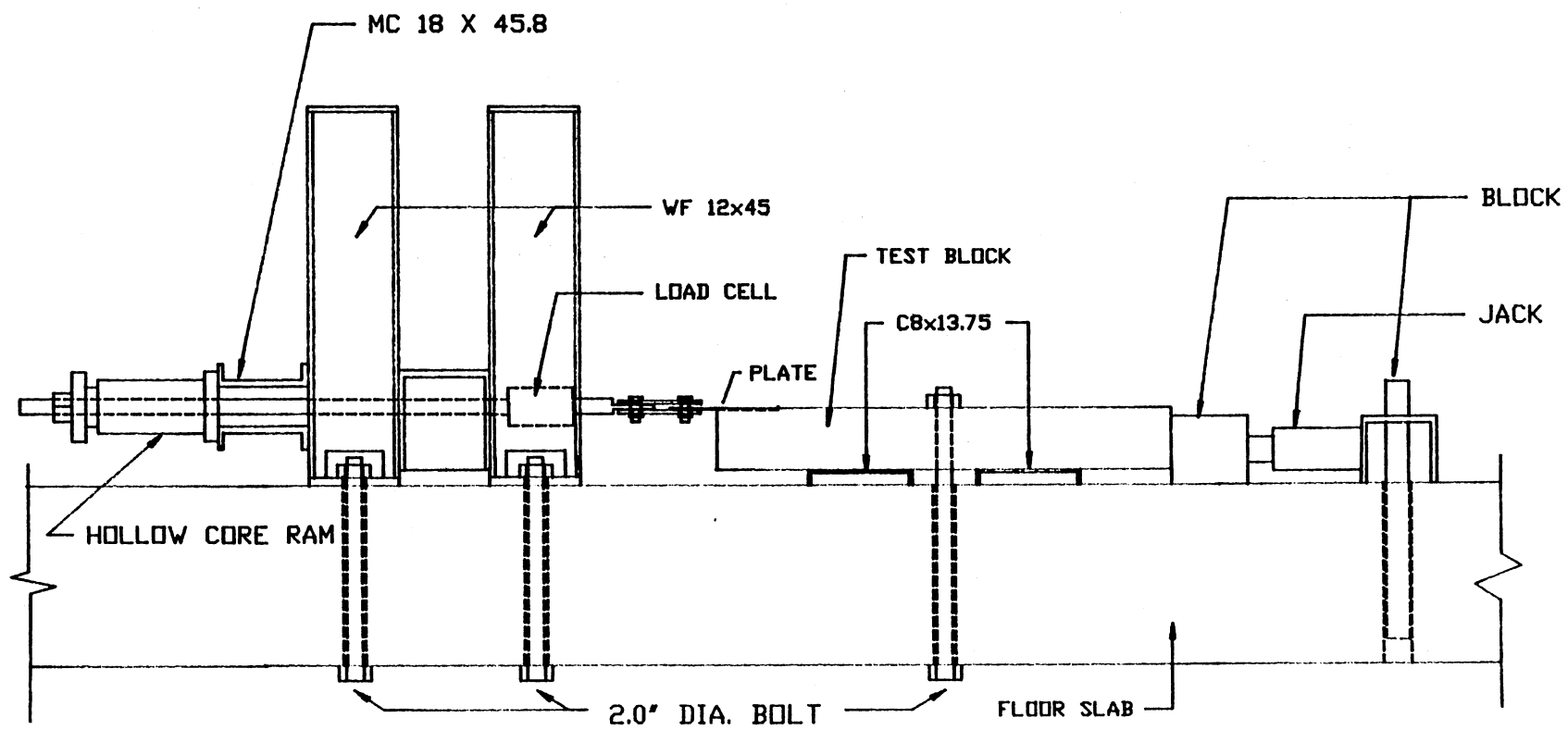


Figure 12 Test Apparatus (Section)

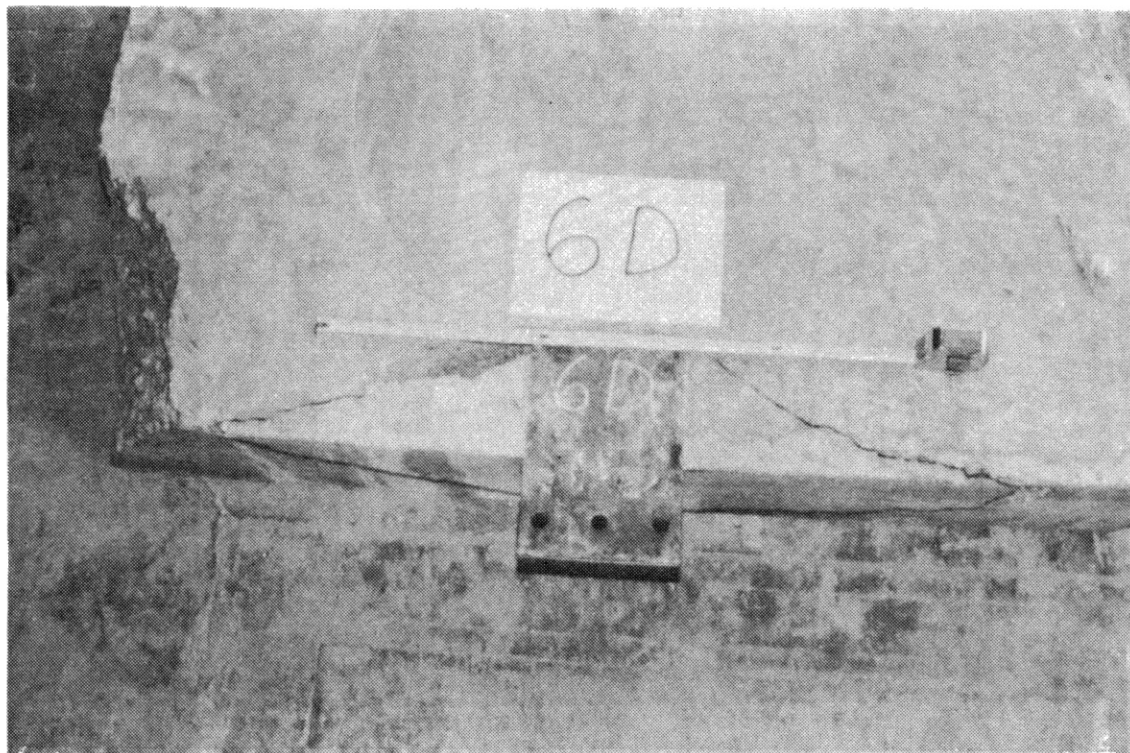


Figure 13 Semi-conical Failure Mode for Type I Specimen
Embedded in "Thick" Slab

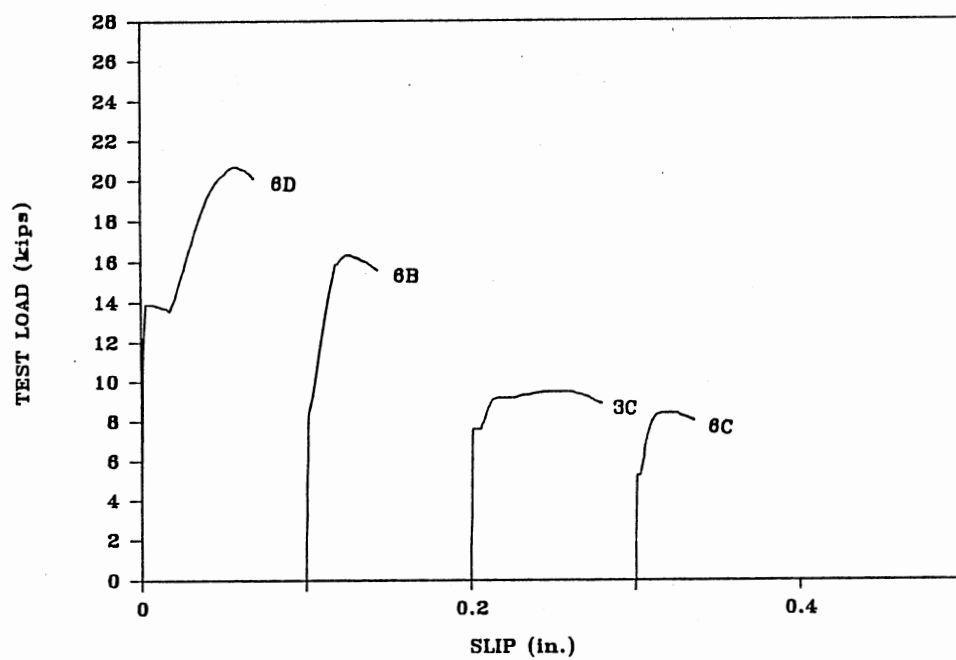


Figure 14 Load-Slip Curves for Type I Specimens Embedded in "Thick" Slabs



Figure 15a Failure Pattern for Type I Specimens Embedded
in "Thin" Slabs



Figure 15b Failure Pattern for Type I Specimens Embedded
in "Thin" Slabs

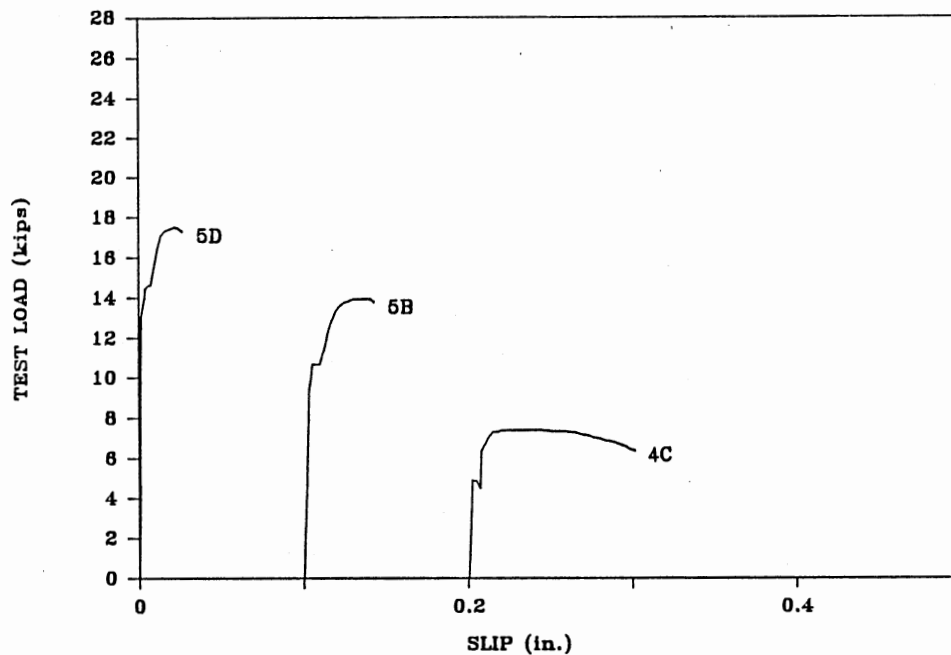


Figure 16 Load-Slip Curves for Type I Specimens Embedded in 4 in. Slabs

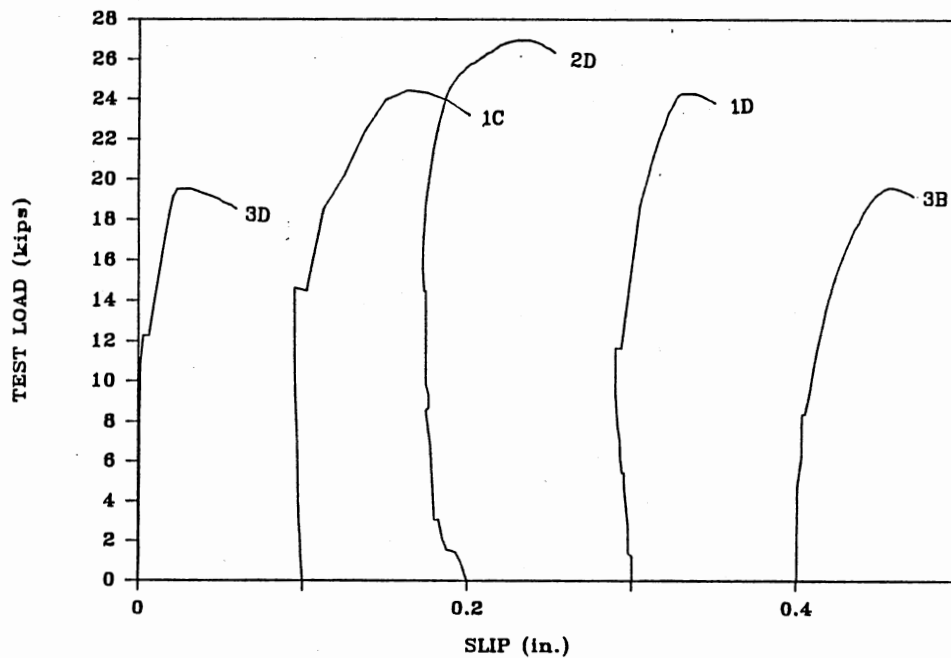


Figure 17 Load-Slip Curves for Type I Specimens Embedded in 8 in. Slabs

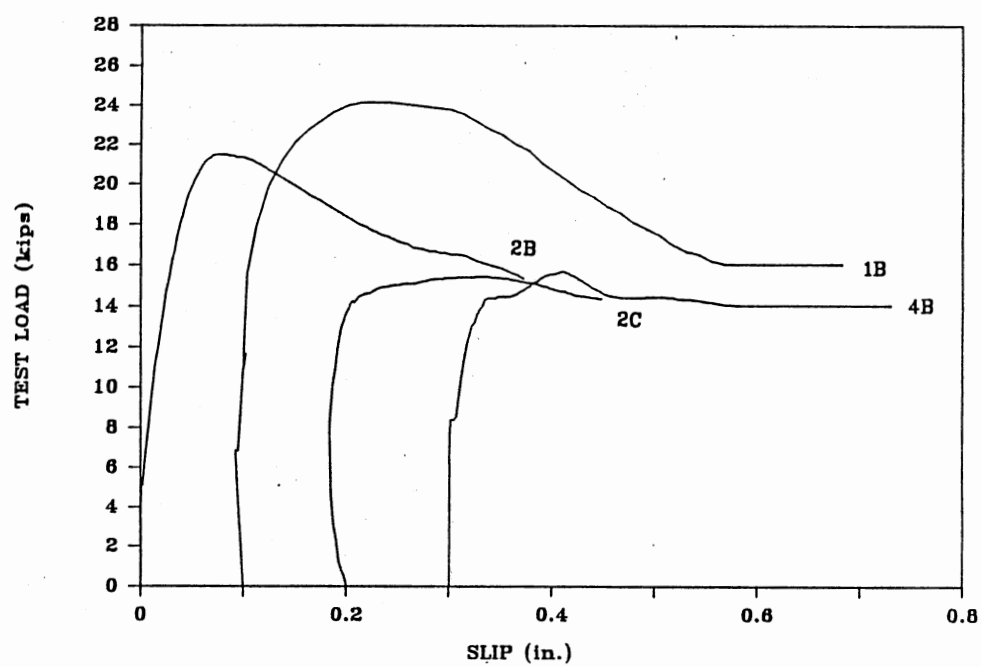


Figure 18 Load-Slip Curves for Type I Specimens with Hairpin Reinforcement

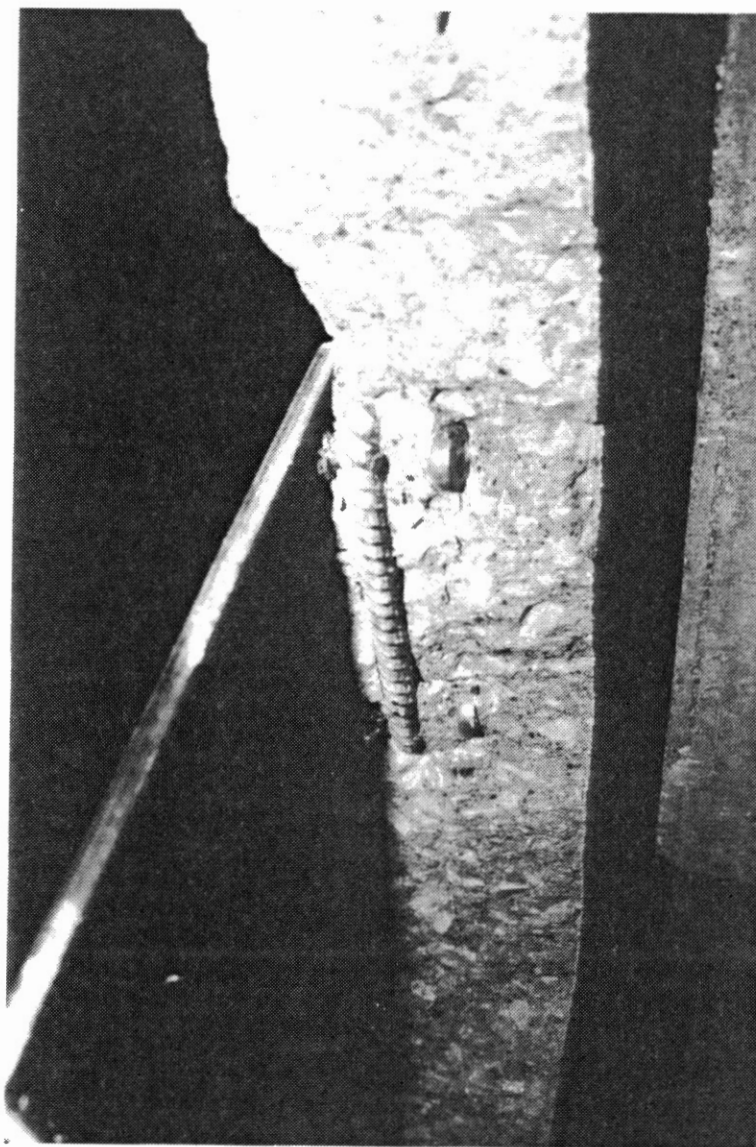


Figure 19 Type I Specimens with Hairpin Reinforcement

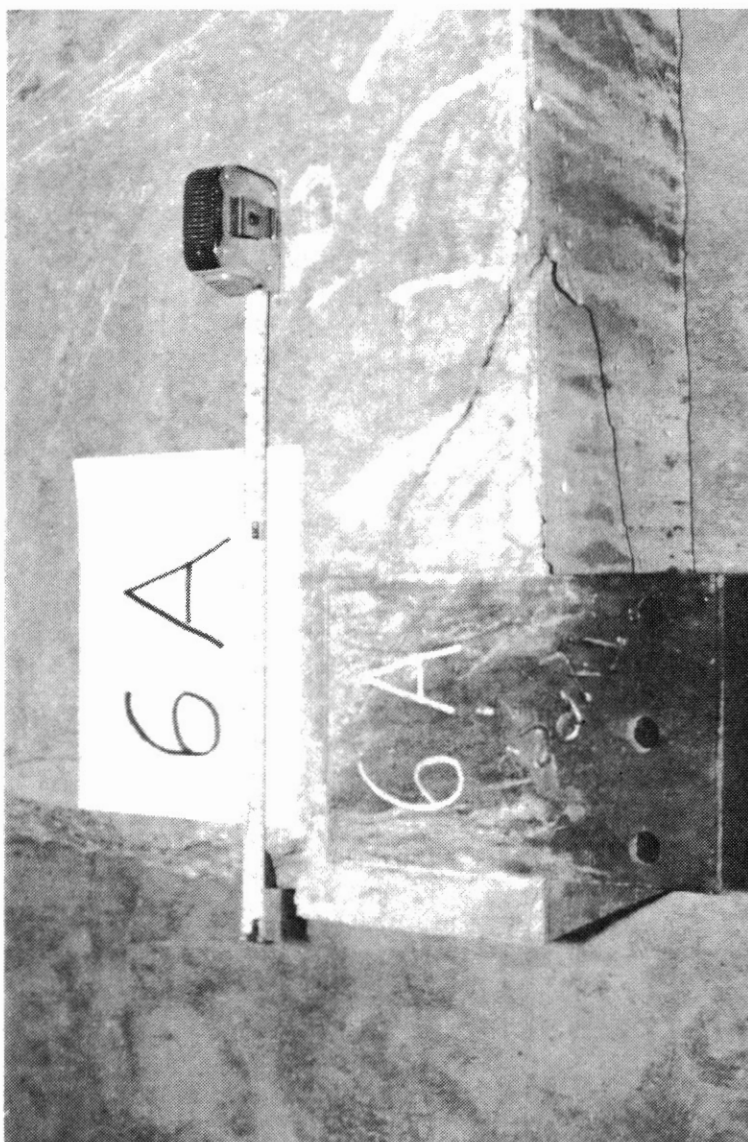


Figure 20 Failure Pattern for Type II Specimens Embedded in "Thick" Slabs

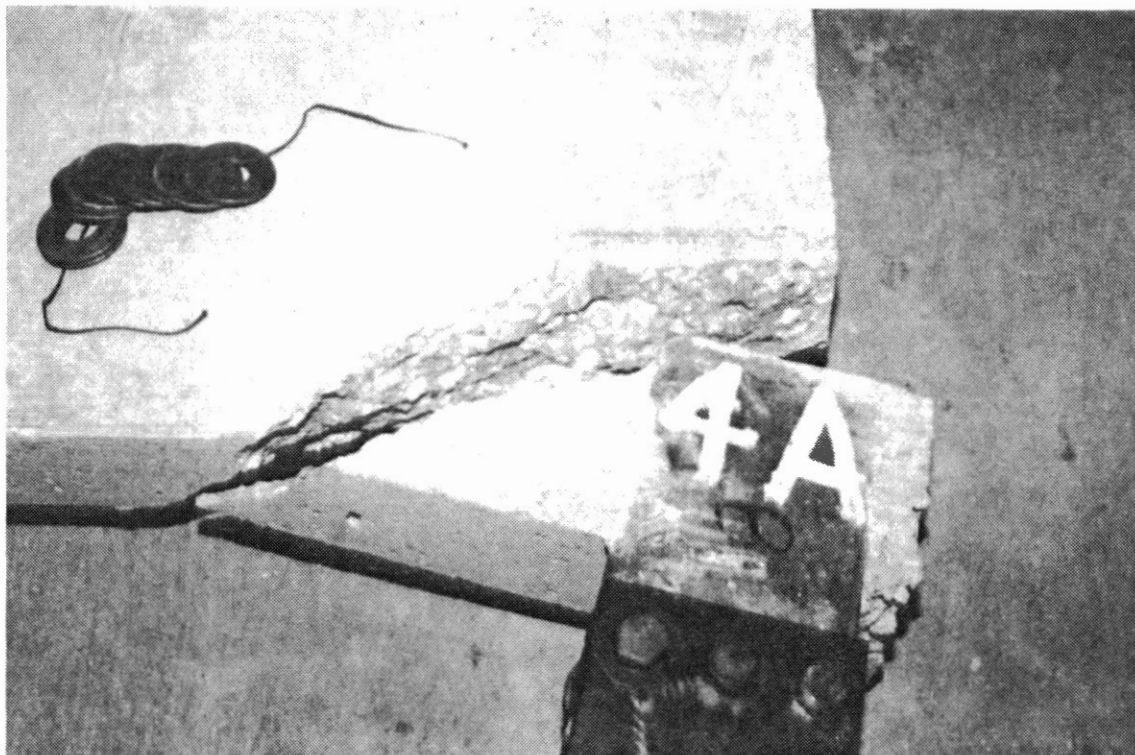


Figure 21 Failure Pattern for Type II Specimens Embedded
in "Thin" Slabs

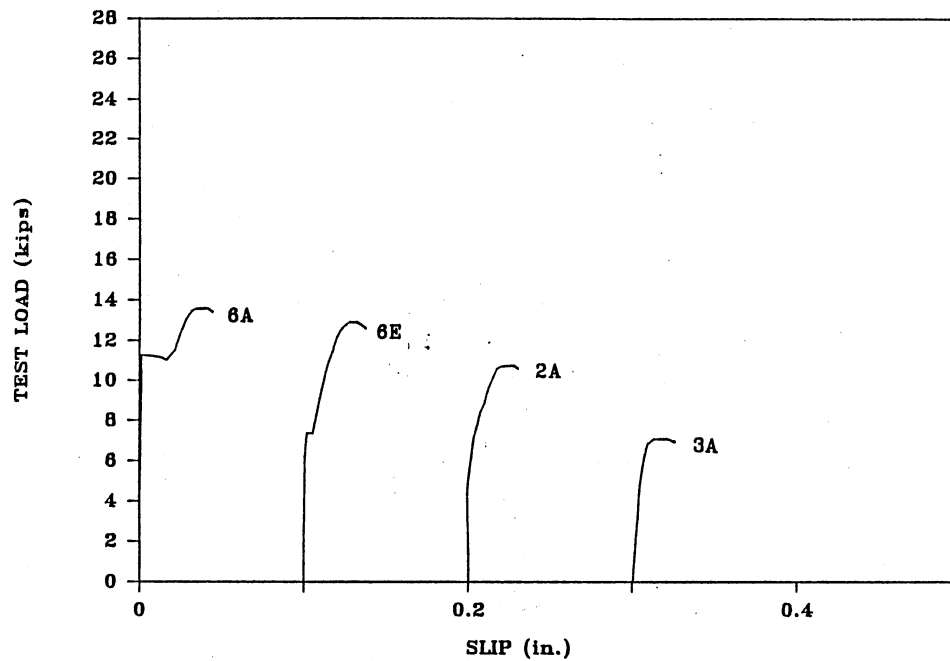


Figure 22 Load-Slip Curves for Type II Specimens Embedded in 12 in. and 8 in. Slabs

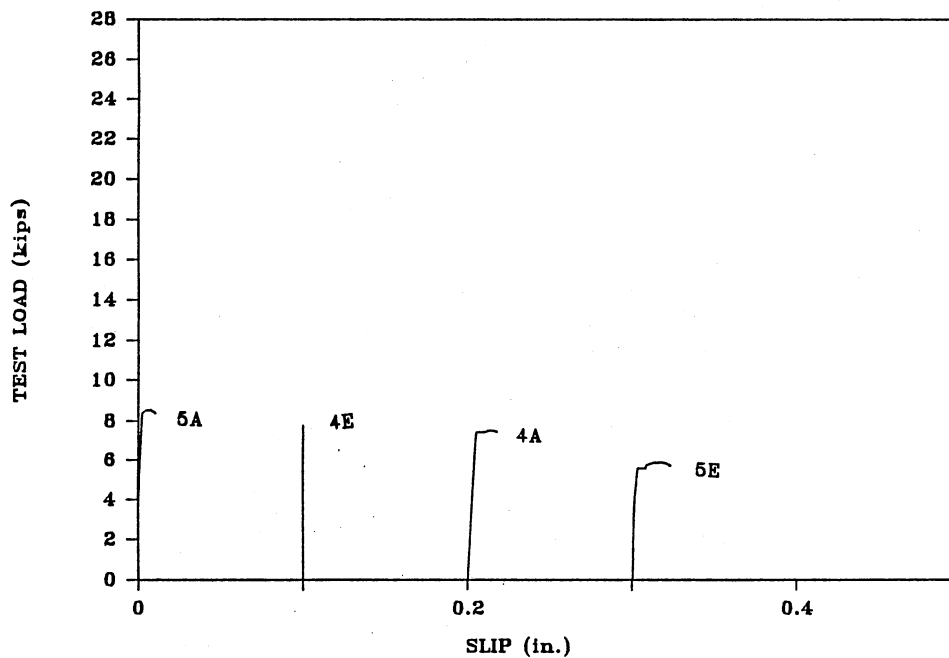


Figure 23 Load-Slip Curves for Type II Specimens Embedded in 4 in. Slabs

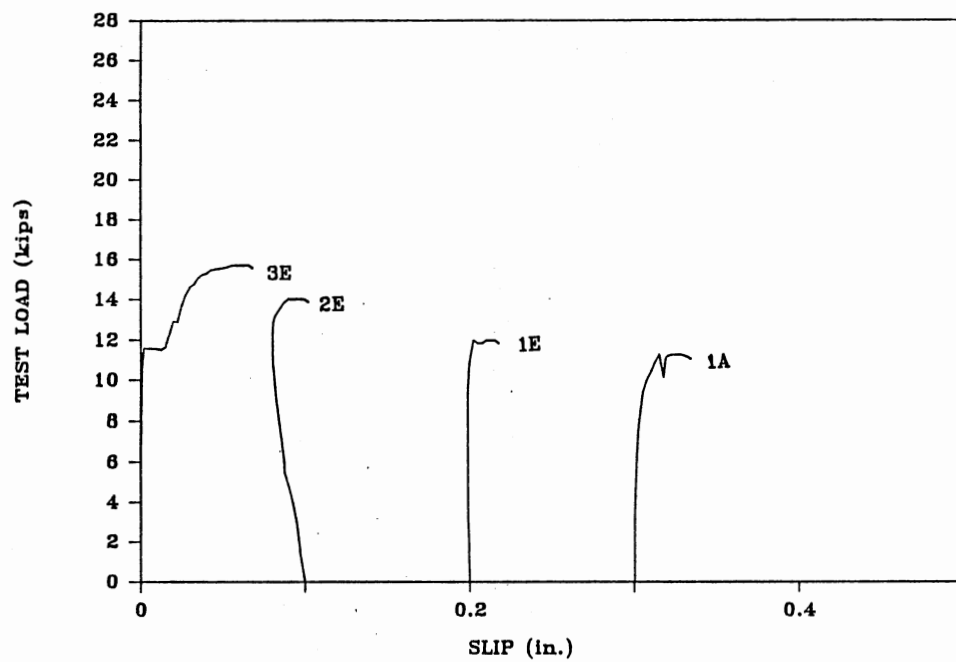


Figure 24 Load-Slip Curves for Type II Specimens
Embedded in 8 in. Slabs

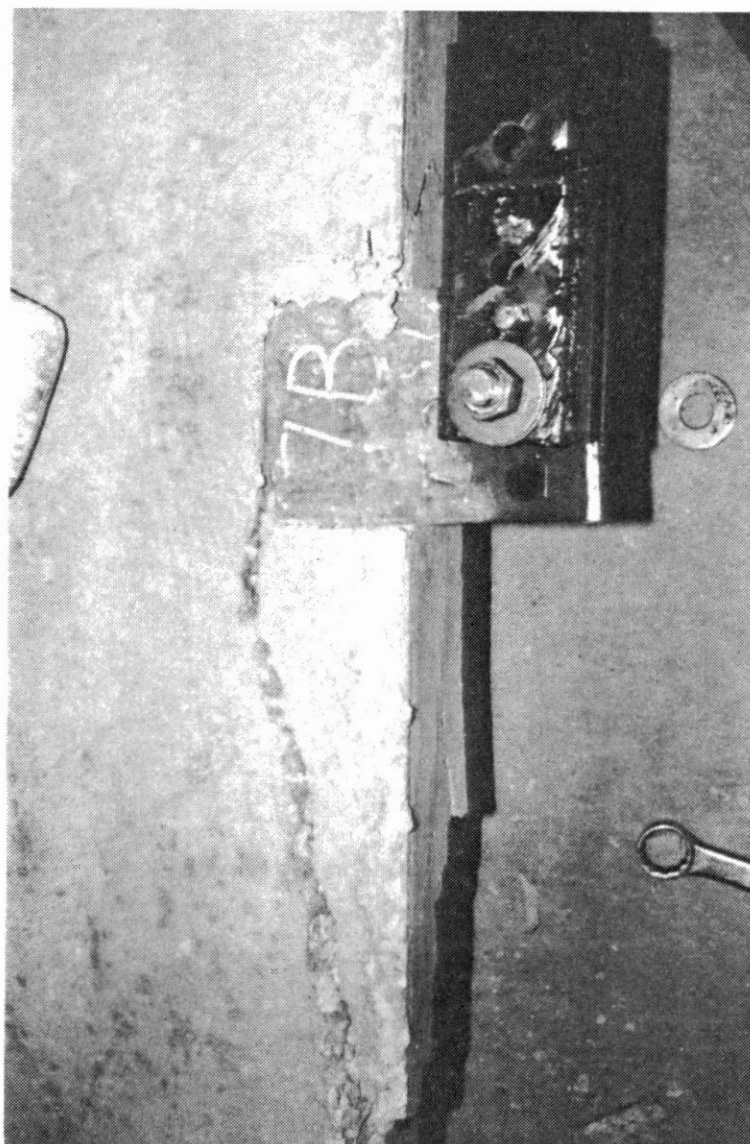


Figure 25 Failure Pattern for Type III Specimens

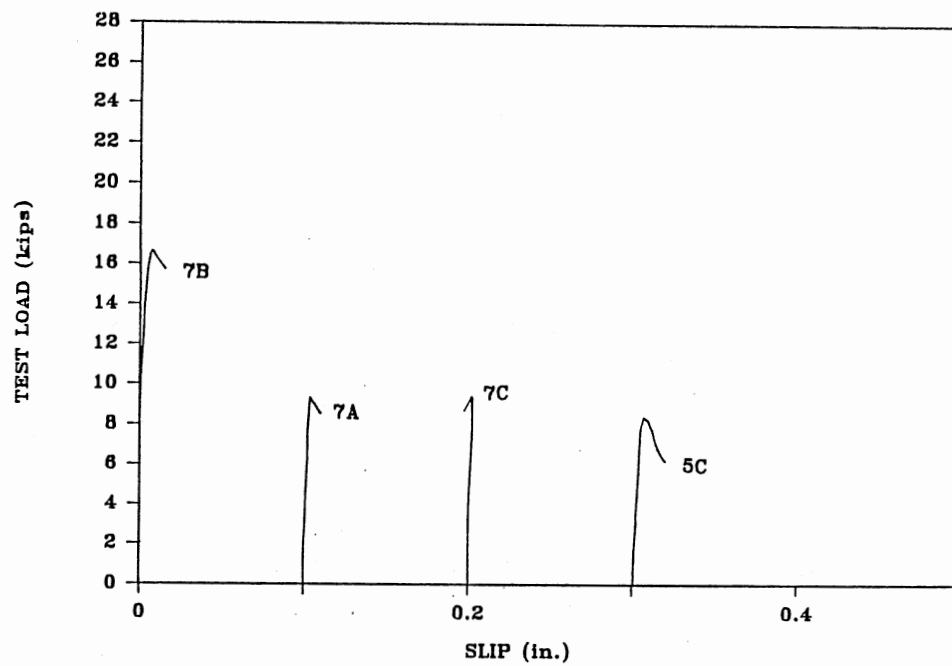


Figure 26 Load-Slip Curves for Type III Specimens

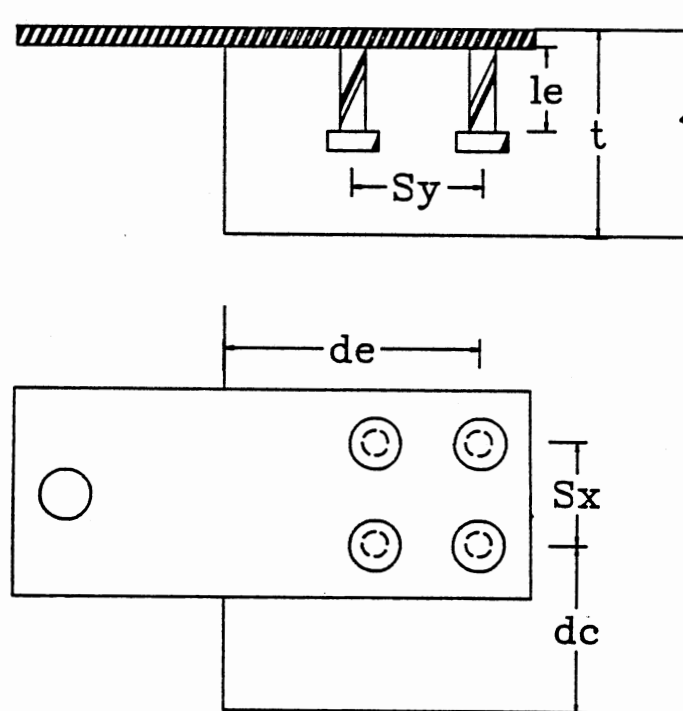


Figure 27 Stud Group Schematic

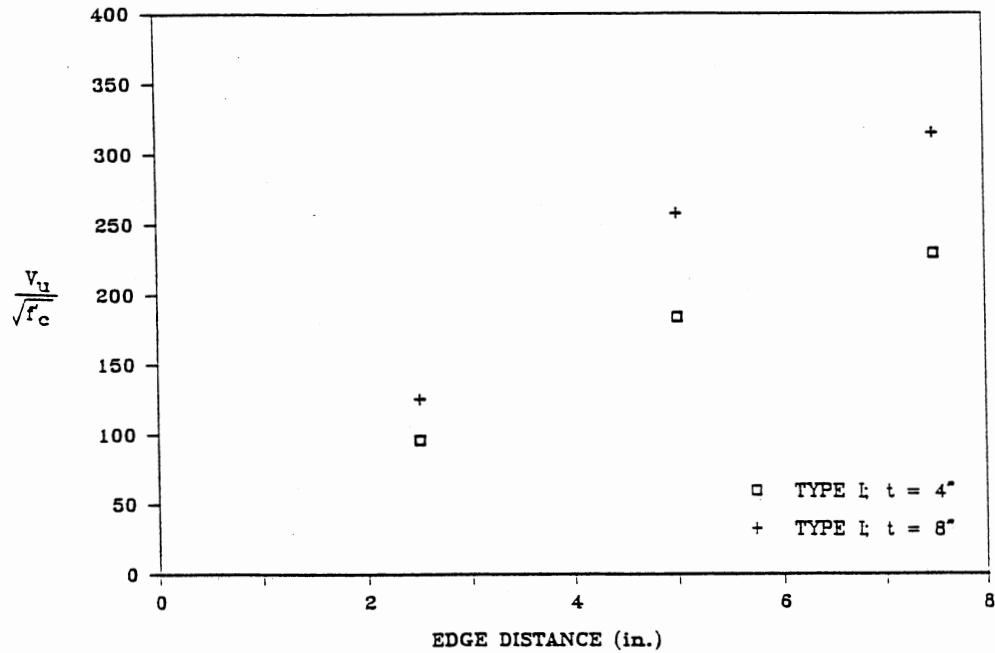


Figure 28 Effect of Edge Distance on Ultimate Test Load for Type I Specimens with 6 in. Stud Spacing

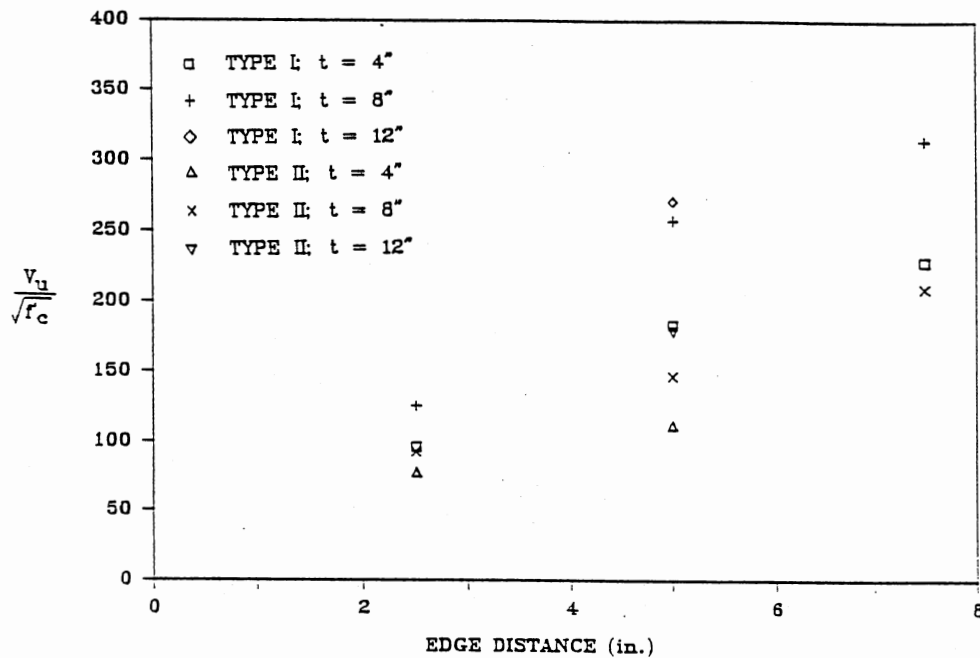


Figure 29 Effect of Edge Distance on Ultimate Test Load for Type I and II Specimens in 4, 8, and 12 in. Slabs with 6 in. Stud Spacing

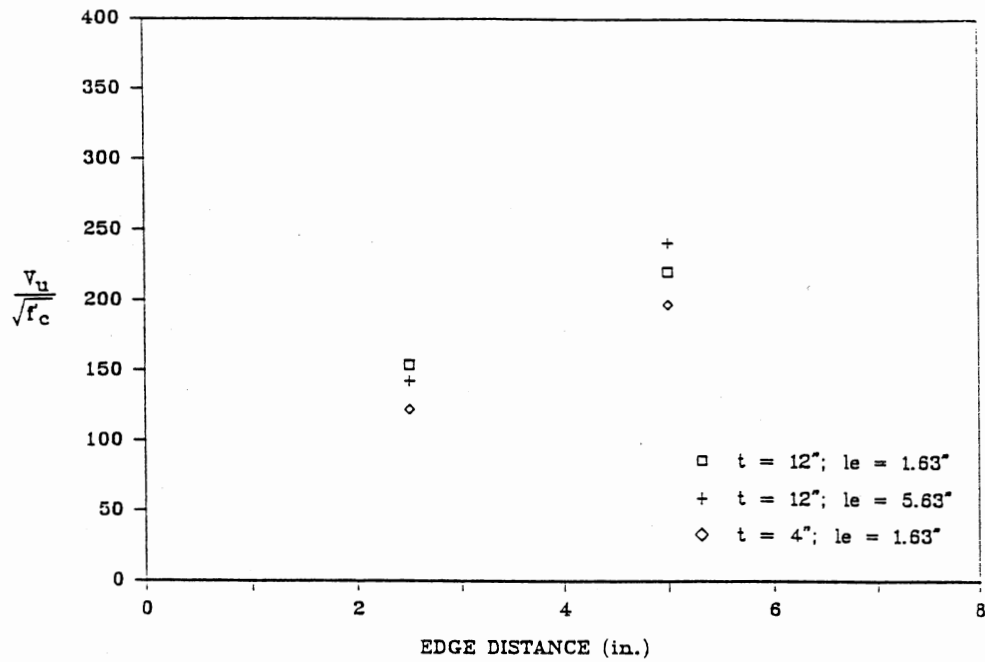


Figure 30 Effect of Edge Distance on Ultimate Test Load for Type III Specimens with 4 in. Stud Spacing

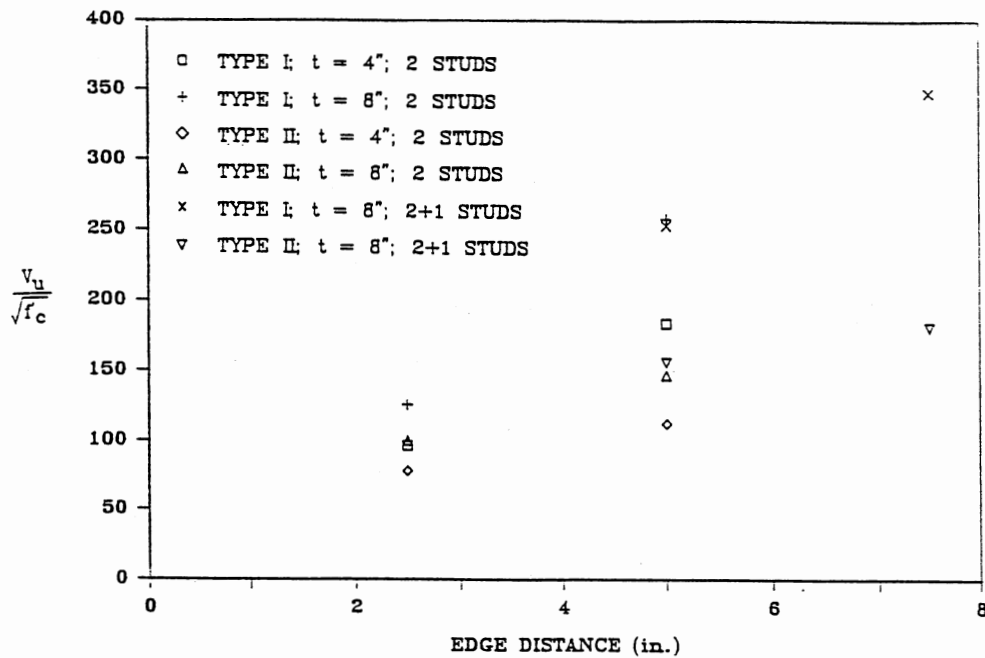


Figure 31 Effect of Corner Distance on Ultimate Test Load for Specimens Embedded in 4 and 8 in. Slabs

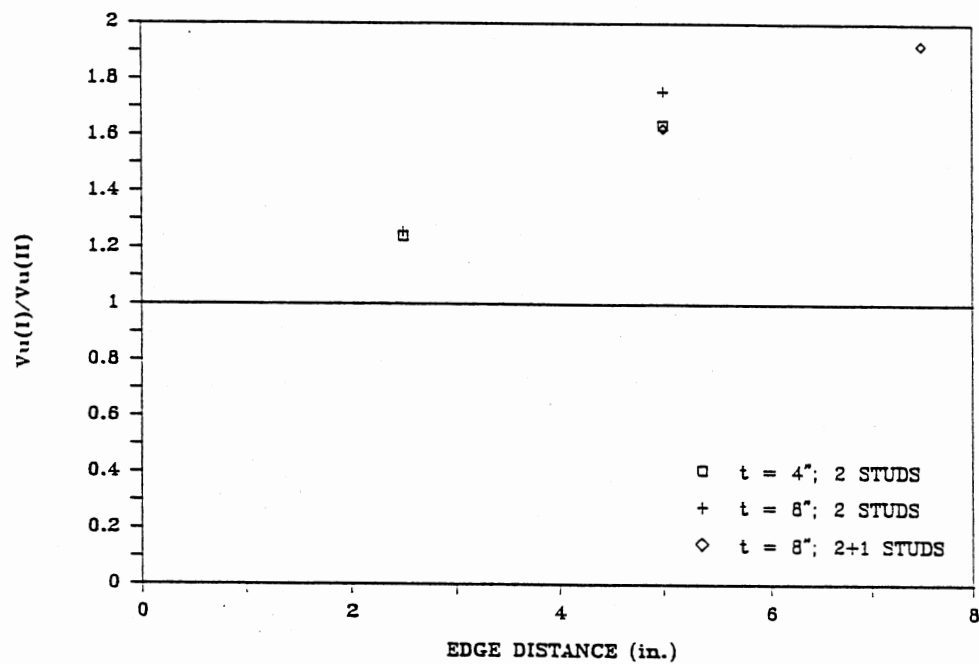


Figure 32 Ratio of Type I to Type II Ultimate Test Load versus Edge Distance

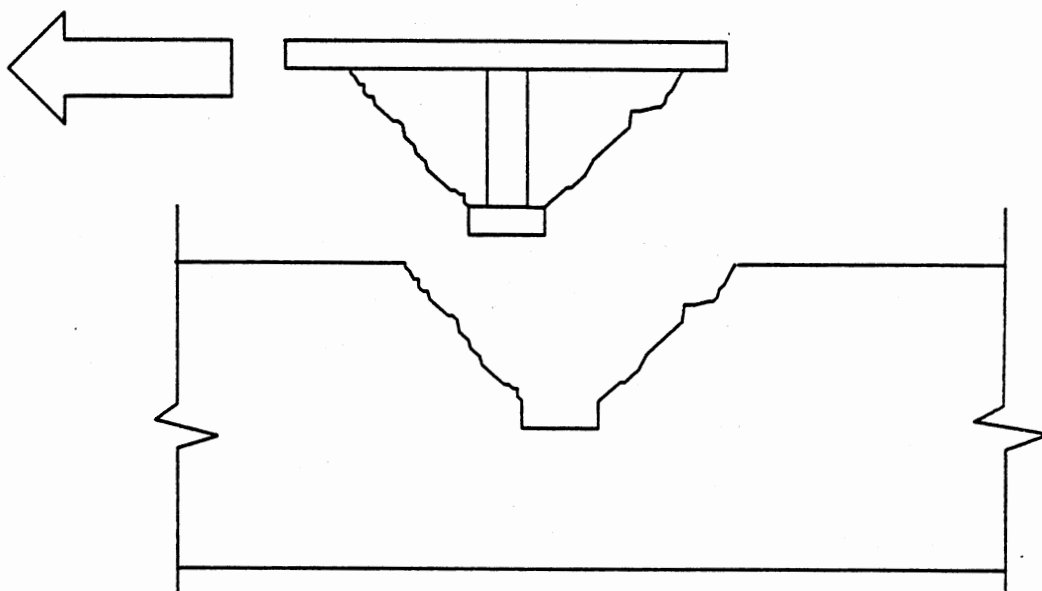


Figure 33 Shear Cone Pullout for a Partially Embedded Stud (19)

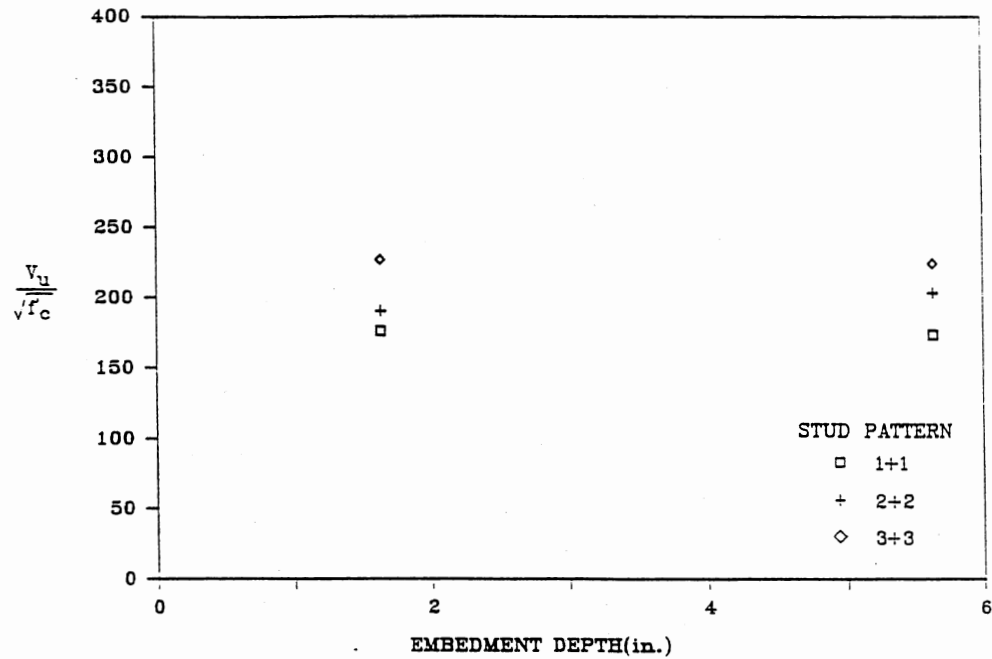


Figure 34 Effect of Embedment Length on Ultimate Test Load for Type I Specimens with Two Rows of Studs (17)

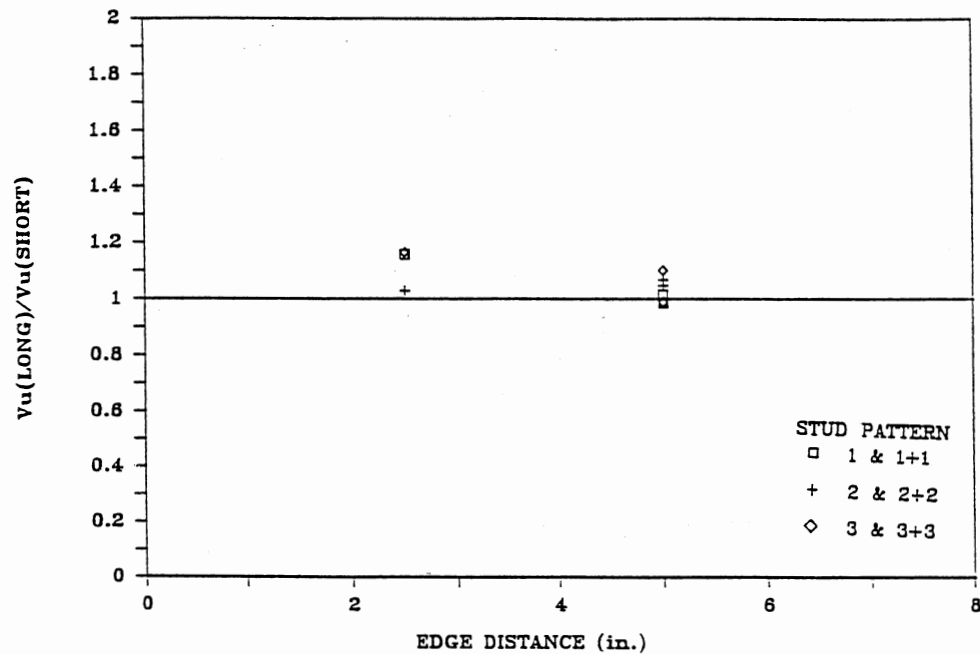


Figure 35 Ratio of Long Stud to Short Stud Ultimate Test Load versus Edge Distance (17)

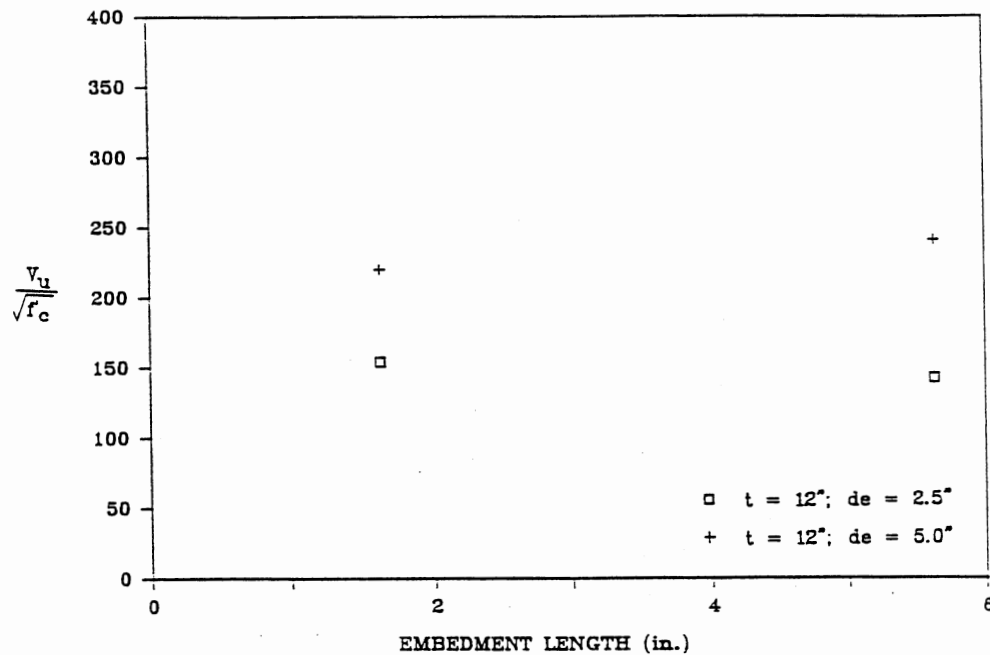


Figure 36 Effect of Embedment Length on Ultimate Test Load for Type III Specimens with 2 in. Stud Spacing (17)

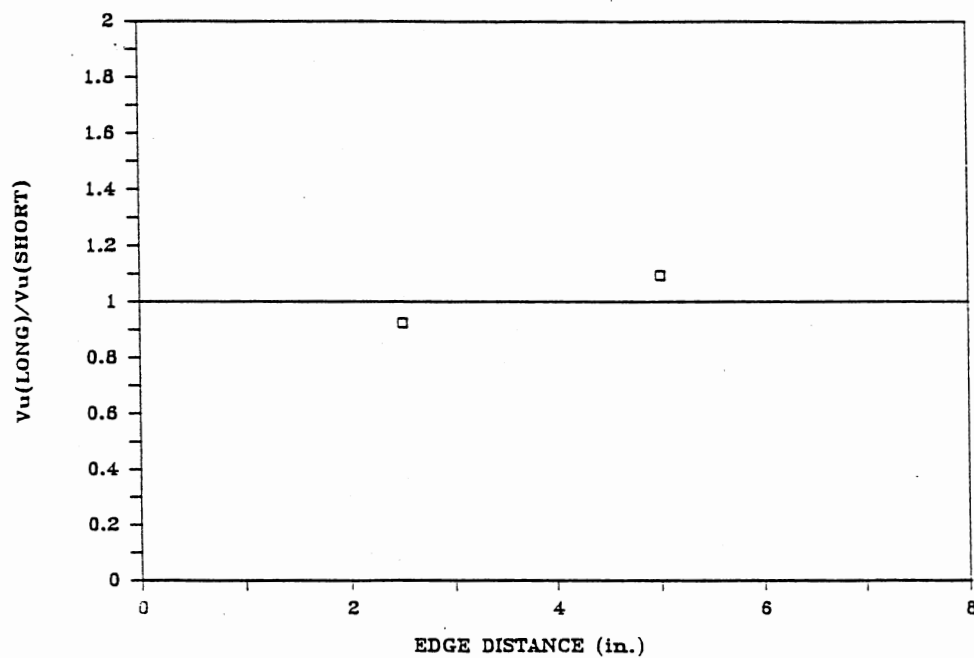


Figure 37 Ratio of Long Stud to Short Stud Ultimate Test Load versus Edge Distance for Type III Specimens with 2 in. Stud Spacing (17)

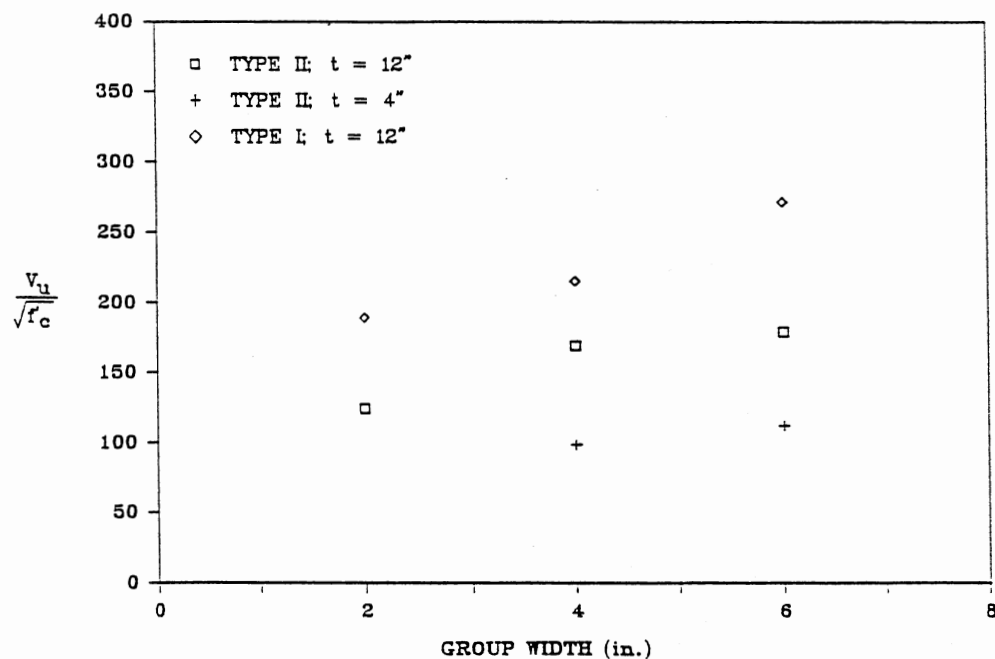


Figure 38 Effect of Lateral Stud Spacing on Ultimate Test Load for Type I and II Specimens with 5 in. Edge Distance

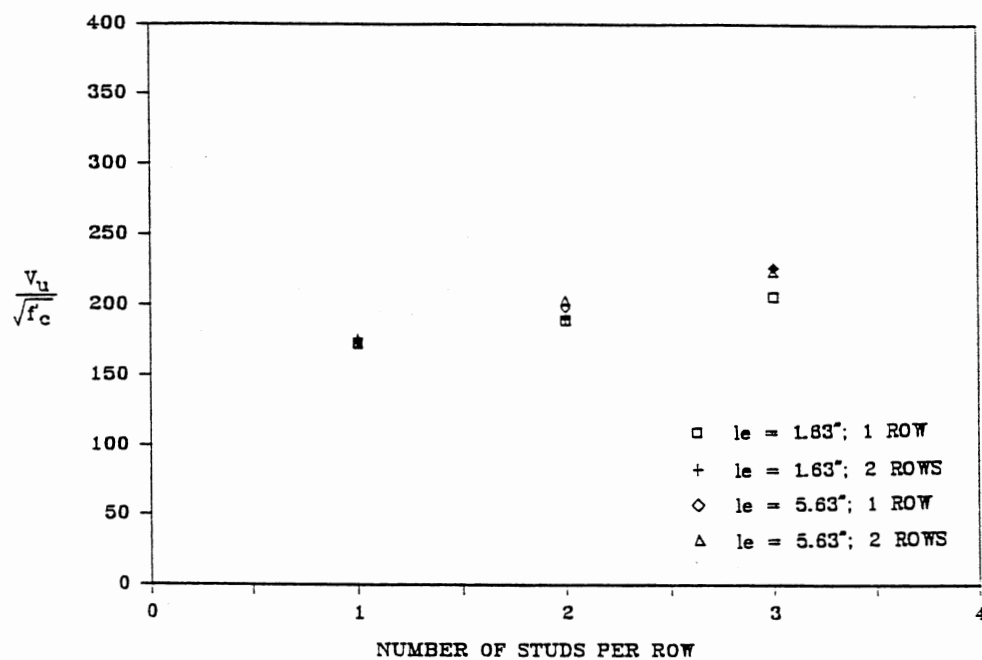


Figure 39 Effect of Front Row Studs on Ultimate Test Load for Type I Specimens with 2 in. Stud Spacing (17)

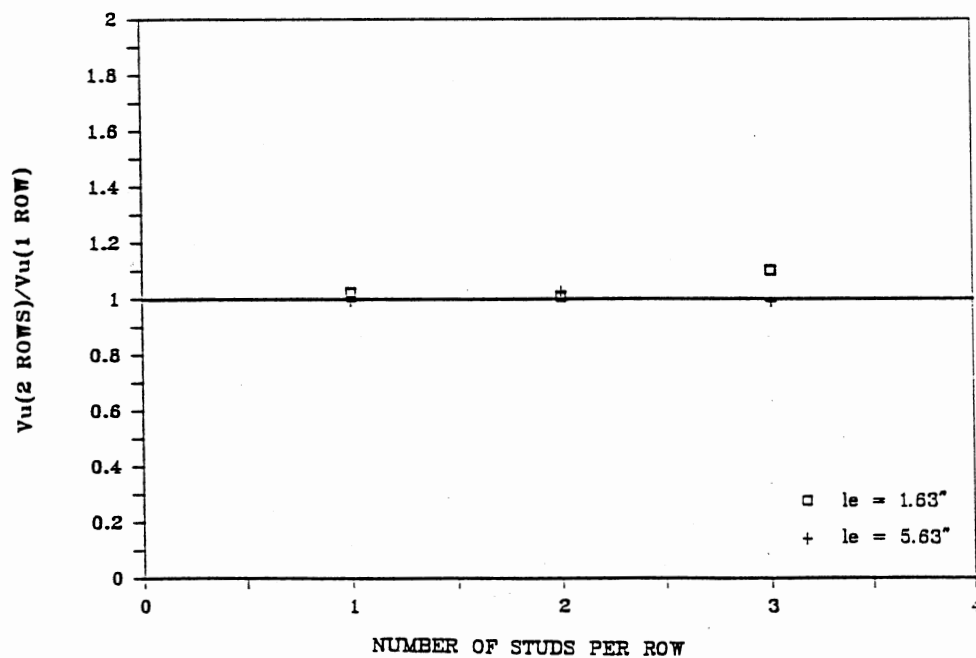


Figure 40 Ratio of Ultimate Test Load for Specimens with Two Rows of Studs to Specimens with One Row versus Number of Studs Per Row (17)

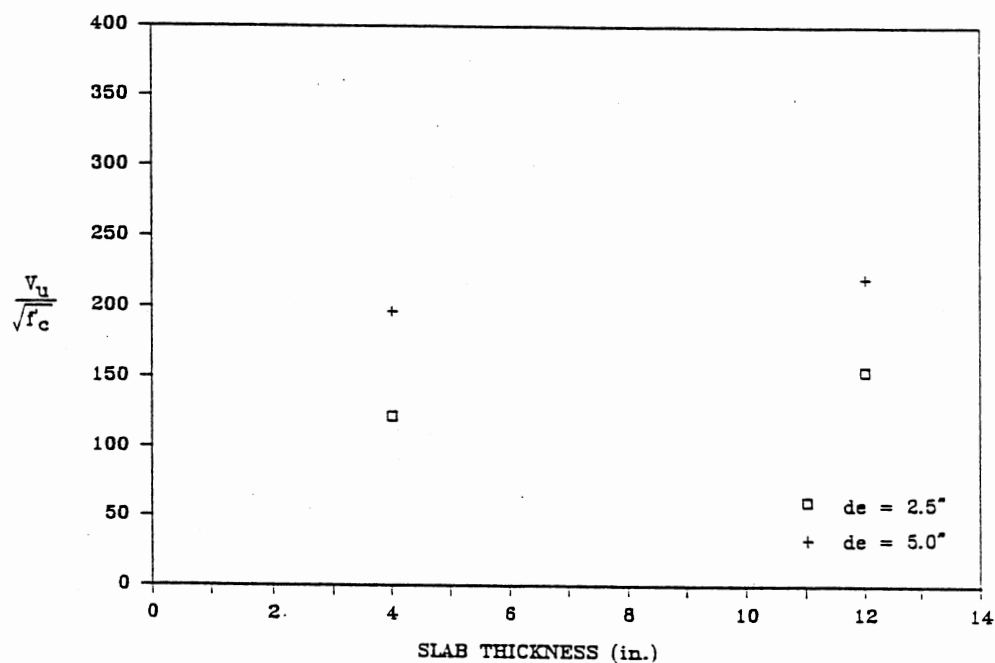


Figure 41 Effect of Slab Thickness on Ultimate Test Load for Type III Specimens with 2 in. Stud Spacing

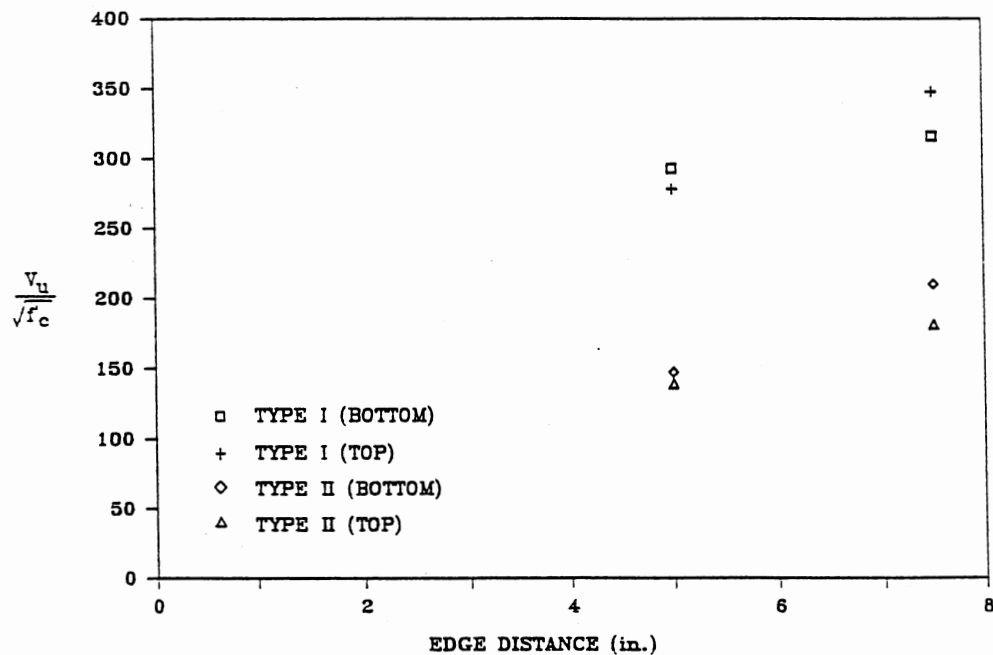


Figure 42 Effect of Casting Position on Ultimate Test Load for Type I Specimens Embedded in 8 in. Slabs with 6 in. Stud Spacing

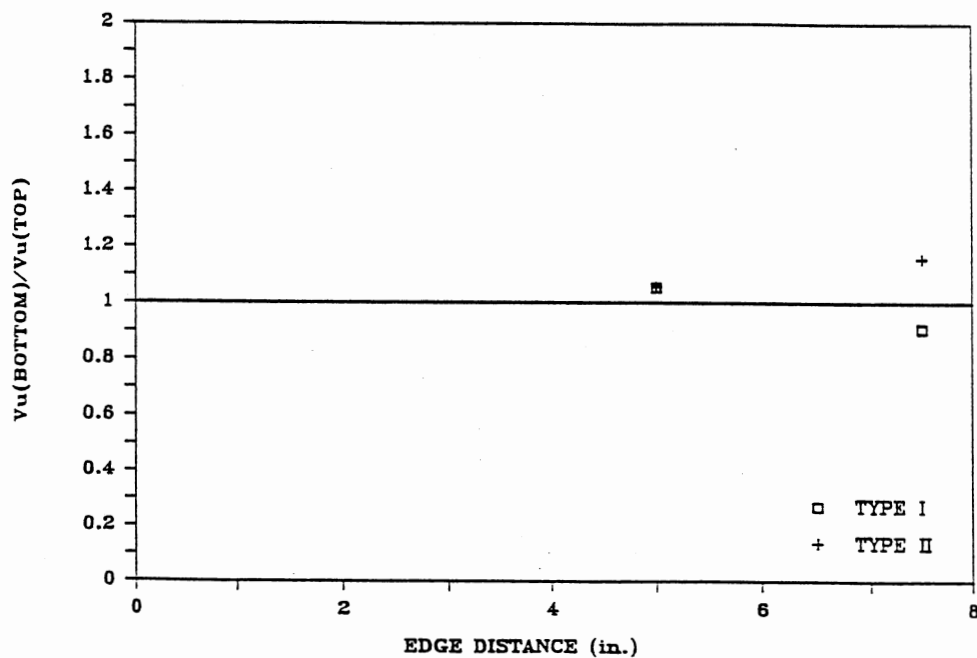


Figure 43 Ratio of Bottom-Mounted Stud Group to Top-Mounted Stud Groups Ultimate Test Load versus Edge Distance

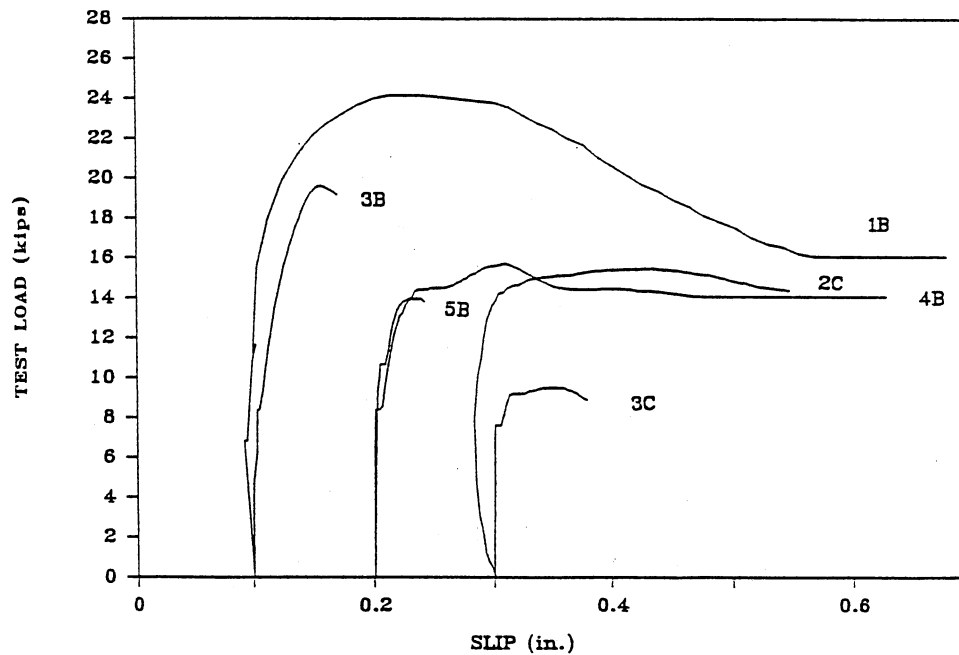


Figure 44 Load-Slip Curves for Specimens with (1B, 4B, and 2C) and without (3B, 5B, and 3C) Hairpin Reinforcement Embedded in 4 and 8 in. Slabs

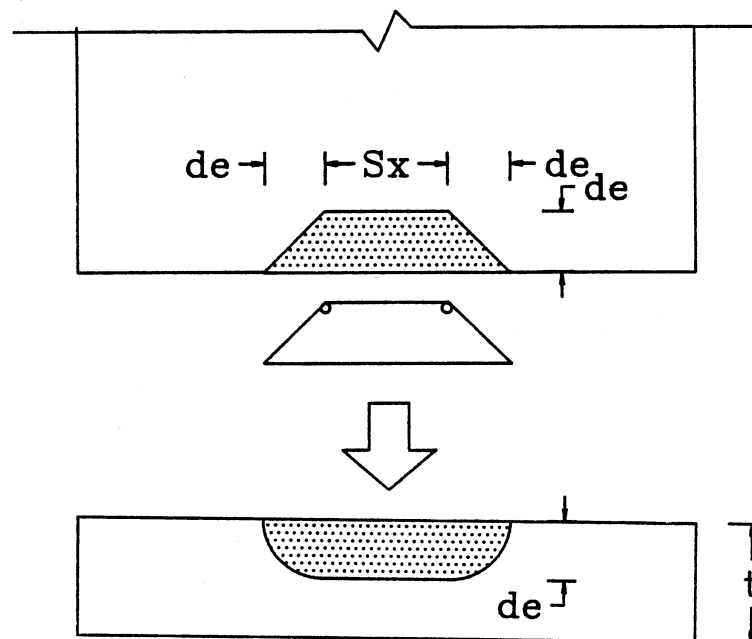


Figure 45 Failure Surface for Type I Specimens Embedded in "Thick" Slabs

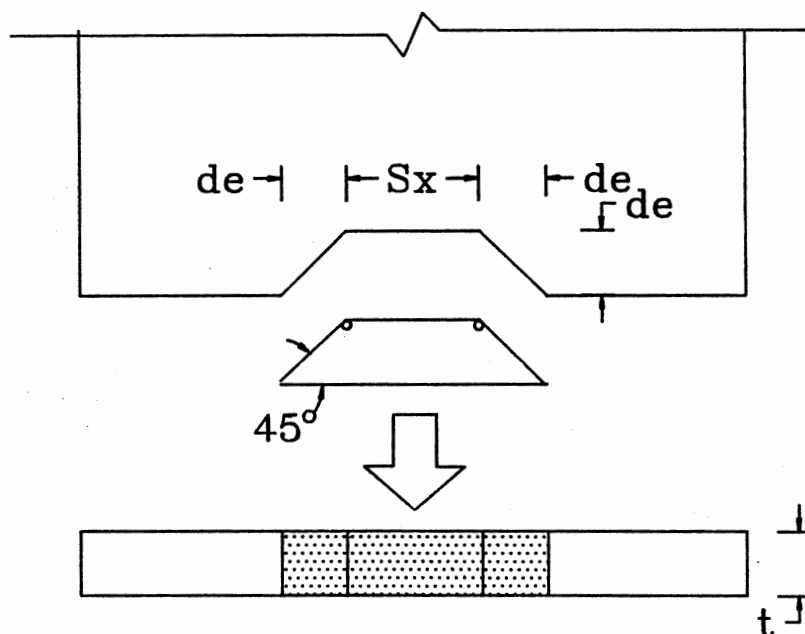


Figure 46 Failure Surface for Type I Specimens Embedded in "Thin" Slabs

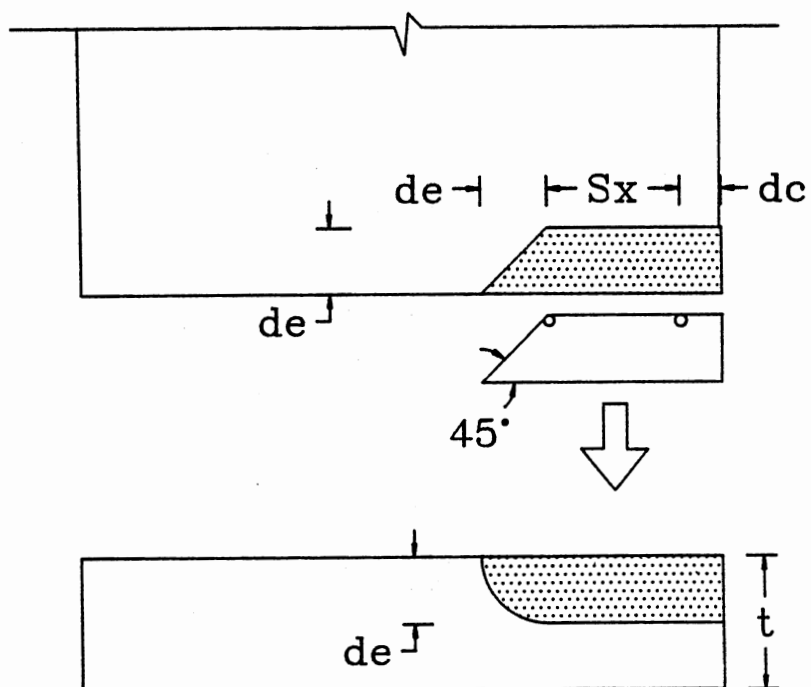


Figure 47 Failure Surface for Type II Specimens Embedded in "Thick" Slabs

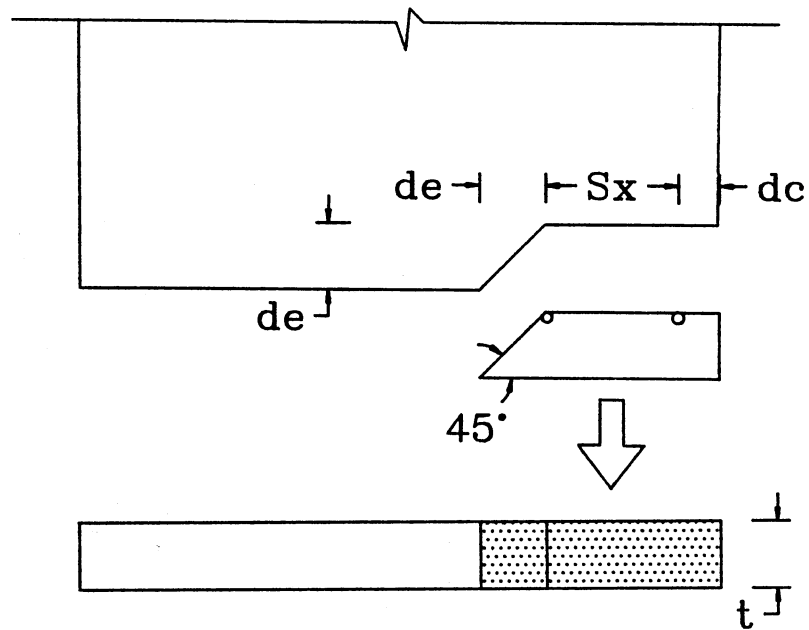


Figure 48 Failure Surface for Type II Specimens Embedded in "Thin" Slabs

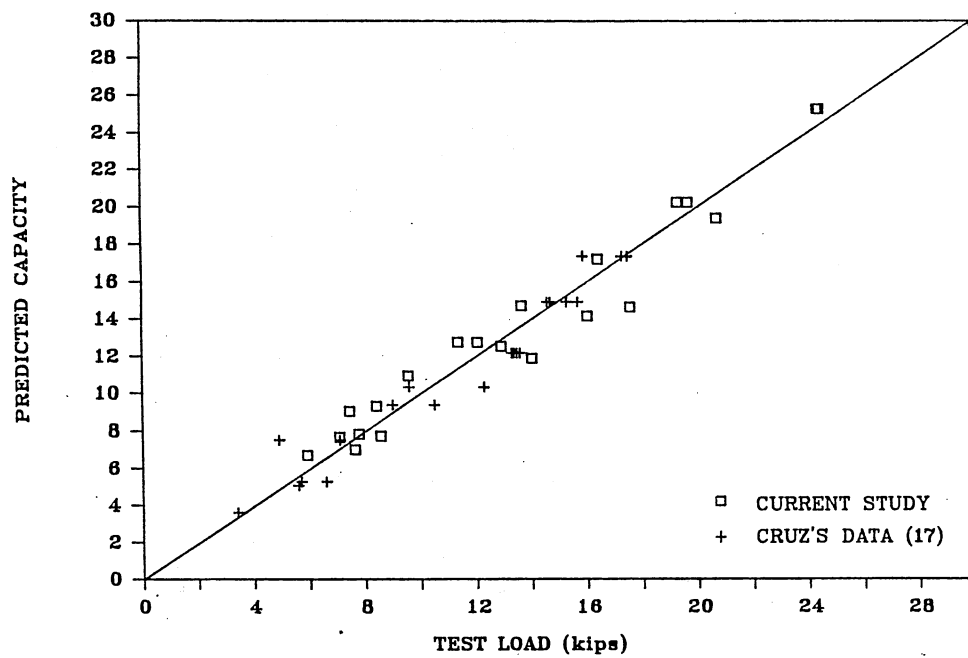


Figure 49 Comparison of Calculated Loads from Eq. 3.4, 3.6, 3.9, and 3.10 with Ultimate Test Loads

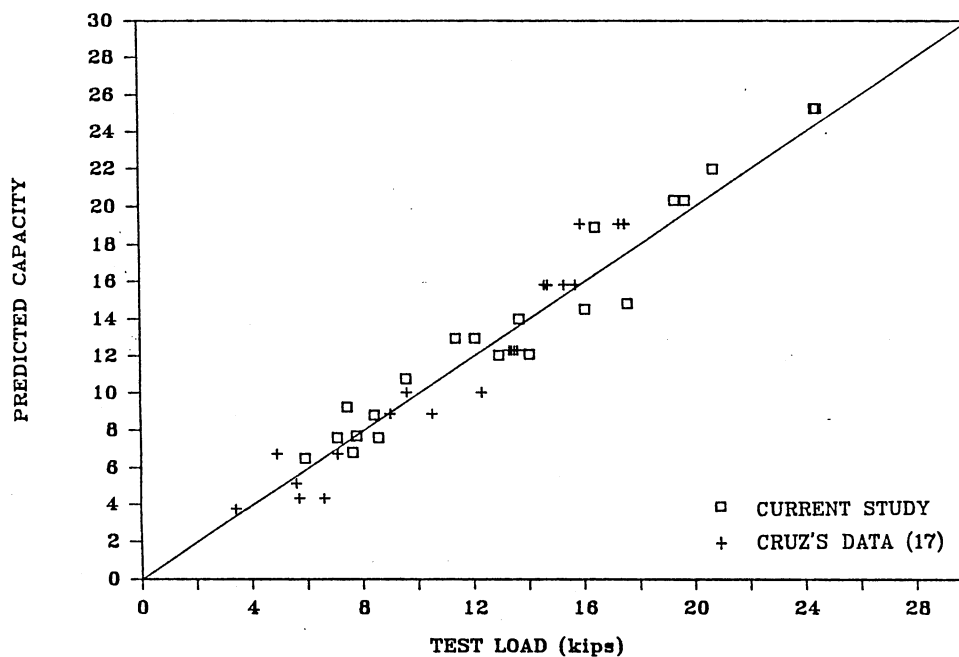


Figure 50 Comparison of Calculated Loads from Proposed Empirical Equations with Ultimate Test Loads

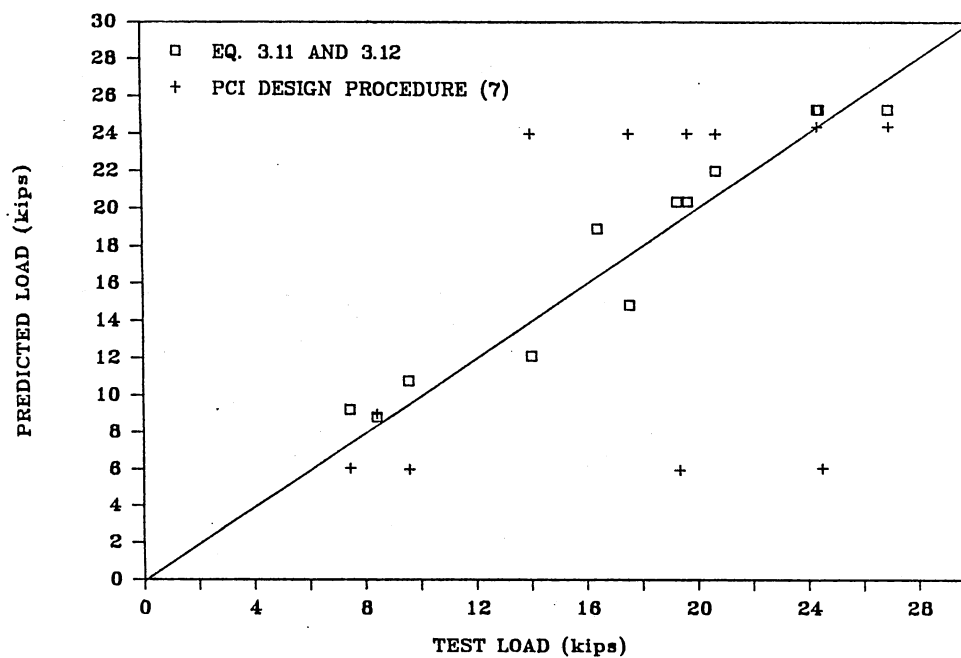


Figure 51 Comparison of Calculated Loads for Type I Specimens Using the PCI Procedure (7) and Proposed Empirical Equations

APPENDIX C

SHEAR TEST DATA (12)

SHEAR TEST DATA (12)

Number	Size	Embed Depth	Edge Distance	Spacing	f'c	Concrete 1000 lbs	Failure Load		Remarks
							Steel 1000 lbs	Per Anchor kips/bolt	
(A307 Bolts)									
1	3/4	6	3	-	5600	11	-	-	#4 HPA
1	3/4	6	6		5700	-	22	22	#6 HPA
1	3/4	6	3		5600	11	22	22	#6 HPA
1	3/4	6	6		5800	17	20	20	#4 HPA
1	3/4	6	3-1/8		3825	9			#6 HPA
1	3/4	6	4-3/16		3825	18	18	18	#6 HPA
1	3/4	6	5		5080	20	20	20	#6 HPA
1	3/4	6	6-3/16		3700		18	18	#6 HPA
1	3/4	6	7-3/8		4100		24	24	#6 HPA
1	3/4	6	8-3/16		4100		19	19	#6 HPA
1	3/4	6	9-5/16		4550		18	18	#6 HPA
1	3/4	6	10-3/4		4600		25	25	#6 HPA
4	3/4	6		8	4600		85	21.3	SM
4	3/4	6		8	4500		87	21.8	SM
4	3/4	6		8	5350	40	6	16	GP
4	3/4	6		8	5100	70	110	27.5	EP
4	3/4	6		8	4450	76	112	28	EP & SB
4	3/4	(A325)			2400		182	45.5	SM
4	3/4	(A490)			2400		183	45.8	SM
2	5/8	Studs		4	6000		36	18	EP
3	5/8	Studs		4	4500		51	17	EP
4	5/8	Studs		4	5000		67	16.8	EP
4	5/8	Studs		4	4500	60	73	18.3	EP
4	5/8	Studs		4	3900	60	65	16.3	EP

SHEAR TEST DATA (12) (continued)

Number	Size	Embed Depth	Edge Distance	Spacing	f'c	Failure Load			Remarks
						Concrete 1000 lbs	Steel 1000 lbs	Per Anchor kips/bolt	
(A307 Bolts)									
4	3/4	3-1/4	(Exp.)	8	5550		44.4	11.1	SM
4	3/4	3-1/4	(Exp.)	8	5600		49.6	12.4	SM
4	3/4	6	(Exp.)	8	4550		100	25	SM

HPA - Hairpin anchor
 GP - Grouted plate
 SB - Shear Bar
 EP - Embedded plate
 SM - Surface Mounted Plate

APPENDIX D

CRUZ'S EXPERIMENTAL DATA (17)

CRUZ'S EXPERIMENTAL DATA (17)

Specimen Number	Concrete Strength (Ksi)	d (in.)	le (in.)	Number Back Row	of Studs Front Row	Sx (in.)	Sy (in.)	t (in.)	de (in.)	dc (in.)	Specimen Type	Test Load
1	5.96	1/2	1.63	1	0	0	0	12	2.5		I	5.70
2	"	"	1.63	1	0	0	0	"	5		I	13.30
3	"	"	1.63	1	1	0	2.5	"	5		I	13.60
4	"	"	1.63	2	0	2	0	"	2.5		I	4.90
5	"	"	1.63	2	0	2	0	"	5		I	14.60
6	"	"	1.63	2	2	2	2.5	"	5		I	14.70
7	"	"	1.63	3	0	2	0	"	2.5		I	9.00
8	"	"	1.63	3	0	2	0	"	5		I	15.90
9	"	"	1.63	3	3	2	2.5	"	5		I	17.50
10	"	"	5.63	1	0	0	0	"	2.5		I	6.60
11	"	"	5.63	1	0	0	0	"	5		I	13.50
12	"	"	5.63	1	1	0	2.5	"	5		I	13.40
13	"	"	5.63	2	0	2	0	"	2.5		I	7.10
14	"	"	5.63	2	0	2	0	"	5		I	15.30
15	"	"	5.63	2	2	2	2.5	"	5		I	15.70
16	"	"	5.63	3	0	2	0	"	2.5		I	10.50
17	"	"	5.63	3	0	2	0	"	5		I	17.50
18	"	"	5.63	3	3	2	2.5	"	5		I	17.30
19	"	"	5.63	1	0	0	0	"	2.5	2.5	II	3.40
20	"	"	5.63	2	0	2	0	"	2.5	2.5	II	5.60
21	"	"	5.63	2	0	2	0	"	5	2.5	II	9.60
22	"	"	5.63	2	2	2	2.5	"	5	2.5	II	12.30
23	"	"	1.63	2	0	2	0	"	2.5		III	11.90
24	"	"	5.63	2	0	2	0	"	2.5		III	11.00
25	"	"	1.63	2	2	2	2.5	"	5		III	17.00
26	"	"	5.63	2	2	2	2.5	"	5		III	18.60

APPENDIX E

**PREDICTED LOAD VERSUS TEST LOAD
FOR TYPE I SPECIMENS**

PREDICTED LOAD VERSUS TEST LOAD
FOR TYPE I SPECIMENS

Specimen #	Predicted Load (Kips)		Test Load (Kips)
	PCI (7)	Eq. 3.11 & 3.12	
1C	6.08	25.30	24.47
1D	24.38	25.30	24.39
2D	24.38	25.30	26.96
3B	24.00	20.36	19.71
3C	6.00	10.79	9.58
3D	6.00	20.36	19.33
4C	6.08	9.26	7.45
5B	24.00	12.11	14.03
5D	24.00	14.85	17.58
6B	36.00	18.95	16.44
6C	9.00	8.83	8.42
6D	24.00	22.02	20.73

2
VITA

Tee-Liang Wong

Candidate for the Degree of
Master of Science

Thesis: STUD GROUPS LOADED IN SHEAR

Major Field: Civil Engineering

Biographical:

Personal Data: Born in Kuala Krai, Kelantan, Malaysia,
December 15, 1962, the son of Bok-Dat Wong and Ji-
Lan Chin.

Education: Received Certificate of Building Technology
from Tunku Abdul Rahman College, Kuala Lumpur,
June, 1983; received Bachelor of Science Degree in
Civil Engineering from Oklahoma State University,
May, 1987; completed requirements for Master of
Science Degree at Oklahoma State University in
December, 1988.

Professional Experience: Project Supervisor for Seramik
Torri Sdn. Bhd. August - December, 1983; Teaching
Assistant, January - May 1987; Research Assistant,
July, 1987-date, School of Civil Engineering,
Oklahoma State University.